

AWARD NUMBER: W81XWH-19-1-0672

TITLE: Targeting WNT5A-mediated Therapy Resistance Mechanisms and Tumor Genomic Heterogeneity in Lethal Bone Metastatic Prostate Cancer.

PRINCIPAL INVESTIGATOR: Christina A.M. Jamieson, PhD

CONTRACTING ORGANIZATION: University of California, San Diego

REPORT DATE: OCTOBER 2020

TYPE OF REPORT: ANNUAL

PREPARED FOR: U.S. Army Medical Research and Development Command
Fort Detrick, Maryland 21702-5012

DISTRIBUTION STATEMENT: Approved for Public Release; Distribution Unlimited

The views, opinions and/or findings contained in this report are those of the author(s) and should not be construed as an official Department of the Army position, policy or decision unless so designated by other documentation.

REPORT DOCUMENTATION PAGE			<i>Form Approved</i> OMB No. 0704-0188	
Public reporting burden for this collection of information is estimated to average 1 hour per response, including the time for reviewing instructions, searching existing data sources, gathering and maintaining the data needed, and completing and reviewing this collection of information. Send comments regarding this burden estimate or any other aspect of this collection of information, including suggestions for reducing this burden to Department of Defense, Washington Headquarters Services, Directorate for Information Operations and Reports (0704-0188), 1215 Jefferson Davis Highway, Suite 1204, Arlington, VA 22202-4302. Respondents should be aware that notwithstanding any other provision of law, no person shall be subject to any penalty for failing to comply with a collection of information if it does not display a currently valid OMB control number. PLEASE DO NOT RETURN YOUR FORM TO THE ABOVE ADDRESS.				
1. REPORT DATE OCTOBER 2020		2. REPORT TYPE Annual Technical Report Y1		3. DATES COVERED 30SEPT2019 - 29SEPT2020
4. TITLE AND SUBTITLE Targeting WNT5A-Mediated Therapy Resistance Mechanisms and Tumor Genomic Heterogeneity in Lethal Bone-Metastatic Prostate Cancer			5a. CONTRACT NUMBER PC180705	
			5b. GRANT NUMBER W81XWH-19-1-0672	
			5c. PROGRAM ELEMENT NUMBER	
6. AUTHOR(S) Christina A.M. Jamieson, PhD E-Mail: camjamieson@health.ucsd.edu			5d. PROJECT NUMBER 0011331499	
			5e. TASK NUMBER	
			5f. WORK UNIT NUMBER	
7. PERFORMING ORGANIZATION NAME(S) AND ADDRESS(ES) UNIVERSITY OF CALIFORNIA, SAN DIEGO OFFICE OF CONTRACT & GRANT ADMINISTRATION. CORTLANDT URQUHART, JD, LLM9500 GILMAN DR DEPT 621 LA JOLLA CA 92093-0621			8. PERFORMING ORGANIZATION REPORT NUMBER	
9. SPONSORING / MONITORING AGENCY NAME(S) AND ADDRESS(ES) U.S. Army Medical Research and Development Command Fort Detrick, Maryland 21702-5012			10. SPONSOR/MONITOR'S ACRONYM(S)	
			11. SPONSOR/MONITOR'S REPORT NUMBER(S)	
12. DISTRIBUTION / AVAILABILITY STATEMENT Approved for Public Release; Distribution Unlimited				
13. SUPPLEMENTARY NOTES				
14. ABSTRACT Advanced prostate cancer is usually treated with Androgen deprivation therapy (ADT) which can help maintain remission in patients, however, growth and metastatic spread often recur. Treatments with new mechanisms of action are urgently needed. We are using patient-derived xenograft and PCa cell line models to test mechanism of action of a new therapeutic target: the WNT5A/ROR1 signaling pathway in prostate cancer for which a therapeutic ROR1 inhibitor antibody, Cirmtuzumab, has been developed and clinically tested in CLL and metastatic breast cancer patients. In Y1 of this grant we have shown that ROR1 is expressed at high levels on castration resistant small cell PCa and neuroendocrine PCa (NEPC) models; two of the most lethal forms of prostate cancer for which there are no curative treatments in PCa cell lines and PDX models. Cirmtuzumab has demonstrated efficacy in our patient derived xenograft organoid cultures. We are now performing in vitro and in vivo testing in NEPC cell lines and in our patient-derived xenograft (PDX) mouse models. We have developed immunohistochemistry (IHC) assays to detect ROR1 in patient biopsy samples which will allow us to define the prostate cancer patient population that expressed ROR1 and to be able to evaluate the treatment in patients for a future clinical trial. These studies are will inform us about the appropriate patient populations for treatment and clinical trials. These pre-clinical studies being performed in this grant will support the pending Phase 1B clinical trial (not part of this grant).				
15. SUBJECT TERMS NONE LISTED				
16. SECURITY CLASSIFICATION OF:			17. LIMITATION OF ABSTRACT	18. NUMBER OF PAGES
a. REPORT Unclassified	b. ABSTRACT Unclassified	c. THIS PAGE Unclassified	Unclassified	61
			19a. NAME OF RESPONSIBLE PERSON USAMRMC	
			19b. TELEPHONE NUMBER (include area code)	

TABLE OF CONTENTS

	<u>Page</u>
1. Introduction	4
2. Keywords	4
3. Accomplishments	5-13
4. Impact	14
5. Changes/Problems	15-16
6. Products	17
7. Participants & Other Collaborating Organizations	18
8. Special Reporting Requirements	18
9. Appendices	
a. OPR Memo on PDX and HRPO	19
b. Technical Abstract	20
c. SOW	21-23
d. Manuscript: Lee et al. (pdf Attached)	24-64

1. INTRODUCTION

My research is focused on metastatic prostate cancer, urologic immune-oncology and therapy. My goal is to develop and test new molecularly targeted therapies and immunotherapies to eradicate this lethal disease. The central tenet of my approach is to study and use patient material to generate new models and use them to perform pre-clinical studies for novel treatments as well as to advance understanding of disease mechanisms of resistance. These patient-derived models more accurately replicate and retain the features of the disease tissues, and thus, are more predictive of patient disease responses when used to test therapies. We have developed patient-derived xenograft models for in vivo PDX and in vitro PDX-derived organoids of bone metastatic prostate cancer. We are using these PDX models in this grant to investigate the mechanism of action of WNT5A:ROR1 signaling in metastatic PCa and the anti-ROR1 antibody therapeutic, Cirmtuzumab.

Background-ROR1 as a Target for metastatic prostate cancer

Wnt signaling was originally discovered as a group of signal transduction pathways critical for normal development and physiology (24, 49, 50). Aberrant Wnt signaling and mutations in the pathway were subsequently associated with tumorigenesis, progression, and metastasis in many cancers including prostate cancer (51, 52). Wnt signaling, which is comprised of the canonical (β -catenin dependent) and noncanonical pathways, is frequently altered in prostate cancer (26, 27). Comprehensive sequencing studies in patients with CRPC have identified recurrent molecular alterations in Wnt signaling pathway components in **about 20% of advanced prostate cancer patients (17)**. Analysis of circulating tumor cells (CTCs) from CRPC patients demonstrate **expression of Wnt5A, the prototypical noncanonical Wnt ligand, in >60% of patients with refractory disease (28, 53-56)**.

The Wnt signaling pathway is complex and context-dependent activities of Wnt signaling are mediated via crosstalk between the canonical and noncanonical Wnt signaling. The Wnt pathway interacts with androgen receptor (AR) signaling, a key pathway in prostate cancer pathogenesis (53). **Noncanonical Wnt signaling is mediated in part through ROR1 tyrosine-kinase-like orphan receptor activation by Wnt5A ligand (Fig 2). Investigating Cirmtuzumab, a cancer stem cell targeting antibody therapeutic, for treatment of lethal metastatic prostate cancer.**

Cirmtuzumab was developed here at UCSD for treating chronic lymphocytic leukemia (CLL). It has successfully passed a Phase 1 safety clinical trial with very few side-effects and is showing efficacy in CLL patients. Cirmtuzumab binds to and inhibits ROR1, an embryonic protein which is not expressed on normal tissues but is upregulated in CLL and some solid tumors. Cirmtuzumab is now in a Phase 1 clinical trial for metastatic breast cancer. We discovered that ROR1 and its partner, WNT5A, are present in some therapy-resistant prostate cancers. We are using our patient-derived models to investigate Cirmtuzumab as a treatment for prostate cancer. We were **awarded the Dept. of Defense Prostate Cancer Research Program Impact Award which now funds this research.**

2. KEYWORDS: Bone metastatic prostate cancer, WNT5A, ROR1, Patient derived xenograft, organoid, Castration Resistant Prostate Cancer (CRPC), Neuroendocrine Prostate Cancer (NEPC), Docetaxel, Cirmtuzumab

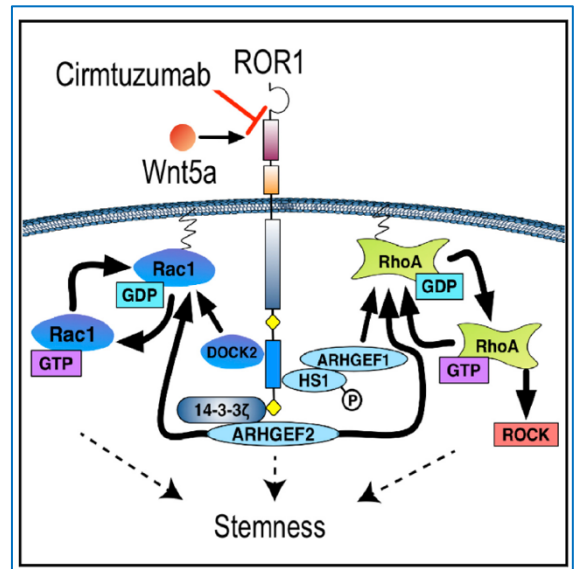


Figure 1. Signaling through the non-canonical Wnt pathway is mediated by Wnt5A binding to its receptor ROR1. Cirmtuzumab is a monoclonal antibody which targets ROR1 (Choi 2018).

3. ACCOMPLISHMENTS

3.1 ACURO approval obtained.

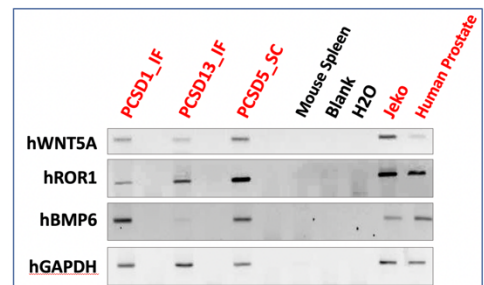
3.2 HRPO not applicable in accordance with ORP_Statement on review of established PDX (Attached as Appendix). The memorandum states: " 2. This memorandum serves to clarify that USAMRDC supported research involving the use of established, existing patient derived xenograft (PDX) models (or the cell lines derived therein) that were established using tissue from deceased donors does not require ORP Human Research Protection Office’s review and oversight for cadaver use in accordance with reference (a).on the use of PDX models." The experiments in our proposal Aims 1 and 2 use PDXs that we established between 2011 and 2014 and have published several publications on from now deceased donors. In Aim 3 we propose to do single cell RNA sequencing of frozen samples from donors who are all deceased.

RESEARCH ACCOMPLISHMENTS - Y1

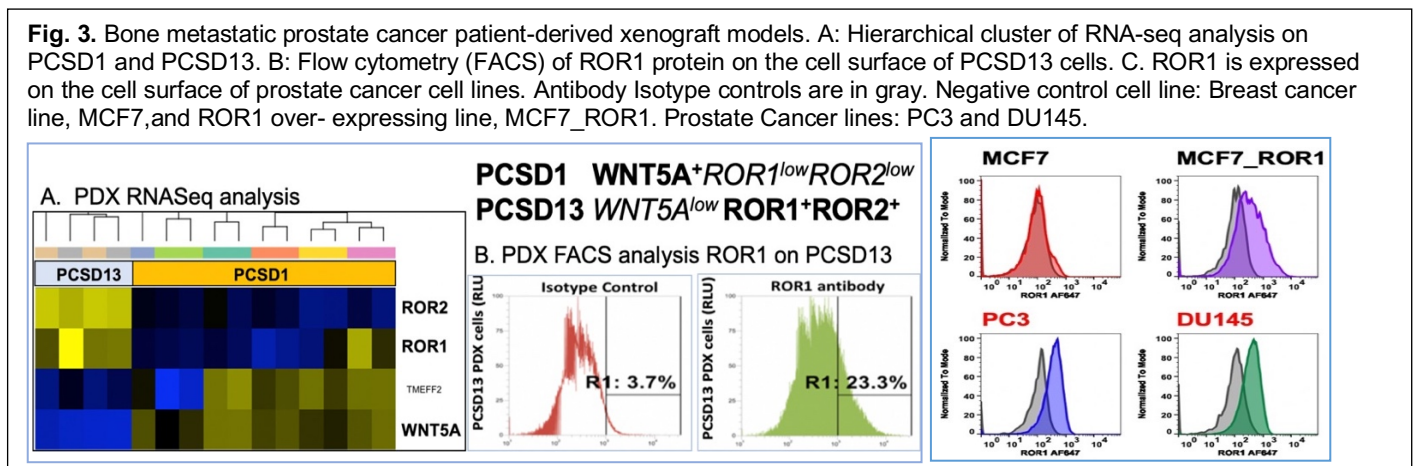
Specific Aim1: Determine the mechanism of WNT5A/ ROR1/ ROR2 signaling in bone metastatic CRPC using patient-derived organoids (PDO) and xenograft (PDX) models using shRNA and small molecule inhibitors of WNT-signaling.

1. ROR1 mRNA is expressed at high levels on castration resistant small cell PCa and neuroendocrine PCa (NEPC) cell lines and TCGA PCa dataset.

PCa bone metastases have been challenging to study because they are not typically surgically removed or biopsied; thus, there are relatively few samples profiled and few models to test new therapies(74-76). The **Jamieson Laboratory** has extensive experience in bone metastasis prostate cancer models. In collaboration with our surgical oncology team, we established a Biobank and new patient- derived xenografts (PDX) named the Prostate Cancer San Diego (**PCSD**) series (77-79). These PDXs closely recapitulate the bone metastatic disease and CRPC in the bone of each patient (77-80). *Patient-derived xenograft and organoid models more accurately represent the patient disease, and thus, testing drugs in these pre-clinical models is more predictive of the patient response and drug efficacy.* Employing these models, we demonstrated key hypothesis-generating findings regarding the interplay between Wnt5A, ROR1/2, and bone metastatic prostate cancer (27). Using whole human genome HTA2.0 Affymetrix microarray and RNASeq gene expression profiling, we found that Wnt5A was highly expressed in a patient prostatic adenocarcinoma bone metastasis specimen and in its corresponding PDX, PCSD1. RT-PCR showed expression of Wnt5a and ROR1 in the PCSD series of PDXs (Fig 2).



RNASeq analysis of patient PCa bone metastasis-derived PDX, PCSD13-a small cell prostate cancer, showed significant ROR1 mRNA expression (**Fig 3A**). Employing FACS analysis, **ROR1 protein** was highly



expressed in PCSD13 cells as well as PC3 and DU145 PCa cell lines (**Fig 3B**). We noted the reciprocal expression of Wnt5a and ROR1 in the bone metastases from the prostate adenocarcinoma, PCSD1, compared to small cell prostate cancer, PCSD13. While **PCSD1**, was PSMA+WNT5A+ROR1^{low}ROR2^{low}, **PCSD13**, was PSMA⁻WNT5A⁻ROR1^{pos}ROR2^{pos}. This may reflect a fundamental difference in prostate adenocarcinoma and prostate small cell carcinoma, or NEPC.

Our findings underscore the need to further characterize ROR1 expression at differential stages in prostate cancer development. Such information will be critical for 1) understanding the role of ROR1 in prostate cancer disease progression and the emergence of neuroendocrine prostate cancer (NEPC), and 2) identifying the most suitable patient population for ROR1 targeting with Cirtuzumab and Cirtuzumab-CART cells.

We performed a search of TCGA prostate cancer RNA expression for ROR1 expression and found that ROR1 was expressed in metastatic PCa and NEPC which represent a minority of the samples in the TCGA database. Interestingly, we also found ROR1 expression was shown in PC3 and DU145 cell lines which are AR negative, NEPC-like cell lines.

2. PCa cell lines, PC3 and DU145, express cell surface ROR1 protein

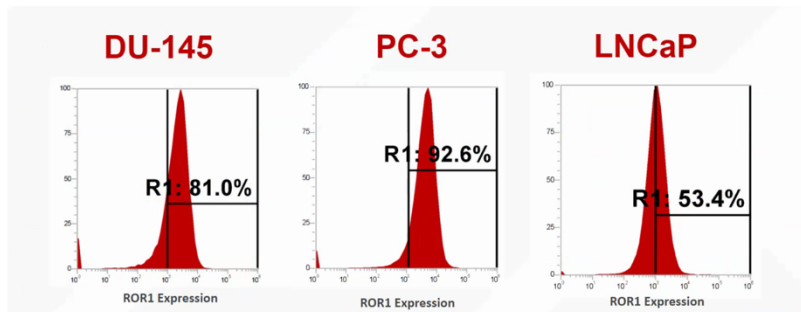
Next we investigated ROR1 expression on PC3, DU145 and LNCaP cells using flow cytometry and showed high ROR1 cell surface protein expressed on PC3 and DU145 comparable to the MCF7-ROR1 overexpressing cell line (Figure).

Defining WNT5A and ROR1 expression in prostate cancer models

a. ROR1 protein expression in flow cytometry: PCSD13, PC3, DU145, LNCaP

Figure 4.

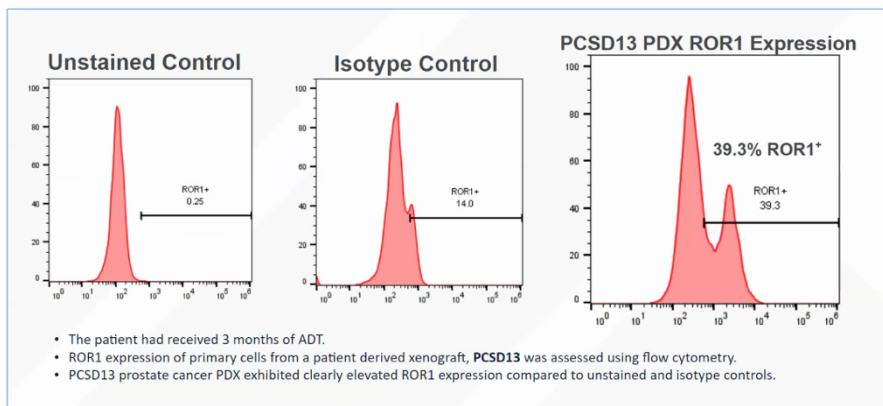
Prostate Cancer (PCa) Cell Lines with High ROR1 Expression:



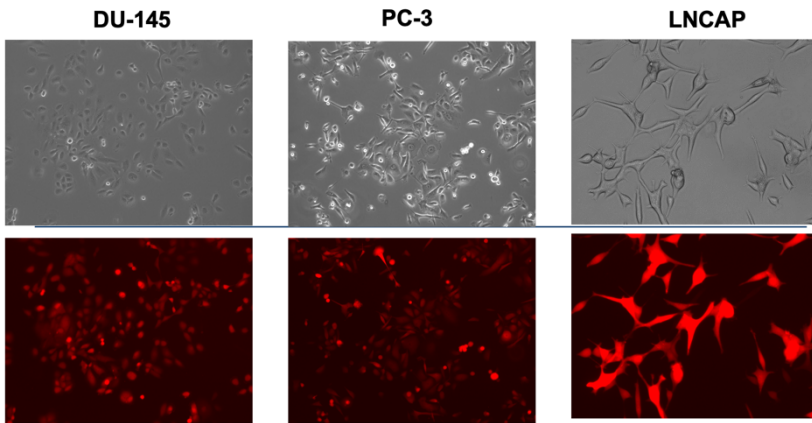
PCa Cell lines DU145 and PC3 have high levels of ROR1 expression as assessed by flow cytometry (Thermo Fisher Attune NxT Flow Cytometry)

Flow cytometry analysis confirmed ROR1 cell surface protein expression on PDX cells from the small cell prostate cancer bone metastasis, PCSD13:

Figure 5. Flow cytometry analysis of cell surface ROR1 protein showed sub-set of ROR1+ cells in PCSD13 PDX tumor cells.



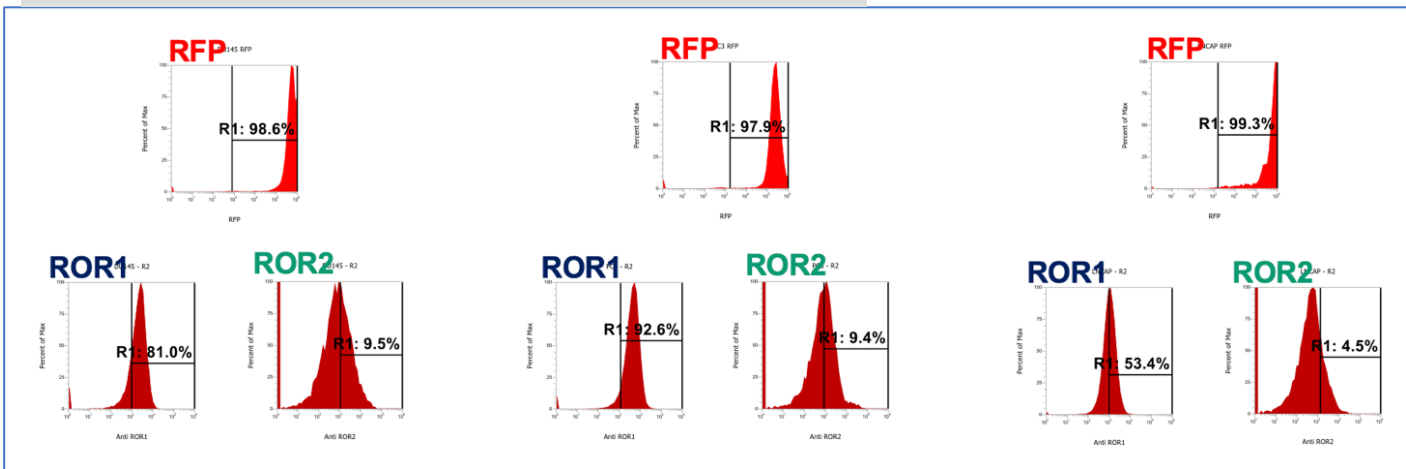
3. Generated PC3, DU145, LNCaP RFP-luciferase expressing cells for in vitro 2D and 3D growth and viability assays for testing Cirmtuzumab and WNT5A in vitro (Incucyte) and in vivo xenograft assays (IVIS).



All Cell lines stably Transduced with RFP-Luciferase lentiviral vector

Figure 6. PCa Cell lines were transduced with RFP-Luciferase lentiviral vector particles express RFP as shown in Incucyte microscope.

Figure 7. Flow cytometry sorting and subsequent analysis was performed on PCa Cell lines transduced with RFP-Luciferase showed high RFP expression on almost 100% of cells. Immunostaining of ROR1 and ROR2 showed high ROR1 staining on PC3 and DU145.



4. Established PC3 PCa cell line organoids (below, left) to study WNT5A:ROR1 signaling and Cirmtuzumab mechanism of action compared to PCSD1 (below, right) and PCSD13 PDX organoids.

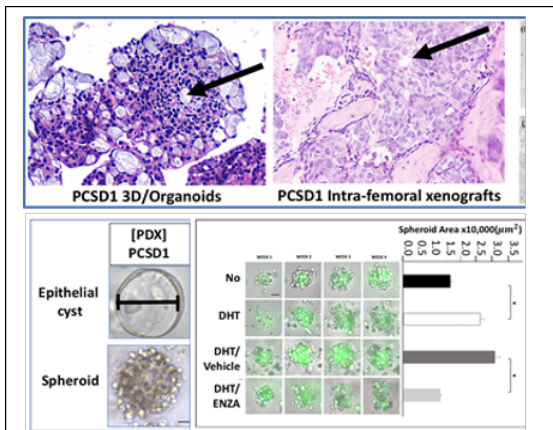


Fig 8. PCSD1 PDX tumors cells form 3D organoids that replicate histomorphology of the xenografts growing in the femur Black Arrows point to these similar structures. Organoids are GFP+.A.PDXs from prostate cancer bone metastases, PCSD1 express GFP-Luciferase B. Enzalutamide PCSD1 reduced lumen size and number of epithelial cysts.

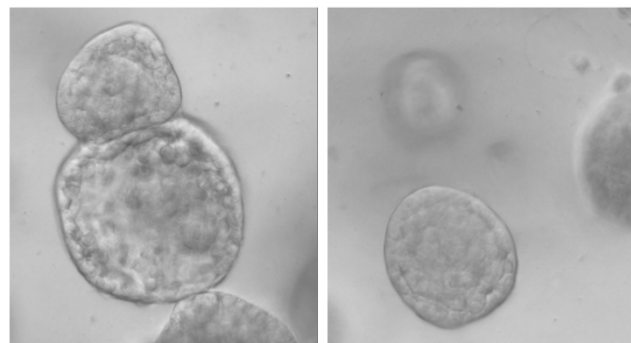


Figure 9. Live microscope images of the PCa Cell line, PC3 organoids grown in 3D optimized PCa organoid conditions (Lee et al 2020).

5. Established Live Cell Cycle Tracking System – The Fucci2BL lentiviral vector for testing cell cycle changes in live organoids was established in PC3, DU145, LNCaP, PCSD1, PCSD13. We are using this to test the cell cycle response to in response to recombinant WNT5A and Cirmtuzumab alone or in combination with This unique system overcomes the limitations of cell cycle analysis as an endpoint and allows for **non-invasive, serial cell cycle analysis in real time in live 3D organoids**.

Standard-of-care therapies: androgen deprivation such as enzalutamide and docetaxel are being tested in our Fucci2BL expressing PCa organoids. The Fucci2BL viral vector and packaged viral particles were obtained as a collaboration with Drs. Gabriel Pineda and Catriona Jamieson, UCSD, and used to transduce PC3, DU145, LNCaP, PCSD1, PCSD13 successfully as shown in **Fig 10** below. PCa cell lines expressing Fucci2BL are shown to have cells in all three of the cell cycle stages: red (G1), yellow (S), and green (G2/M). These cells will be FACS sorted to purify the transduced Fucci2BL cells for use in organoid and xenograft experiments. PCSD1-Fucci2BL cells were used to establish the effects of ADT on cell cycle as shown below and PCSD13-Fucci2BL are now being further FACS sorted and purified for organoids and PDX experiments with WNT5A and Cirmtuzumab alone or in combination with enzalutamide and docetaxel.

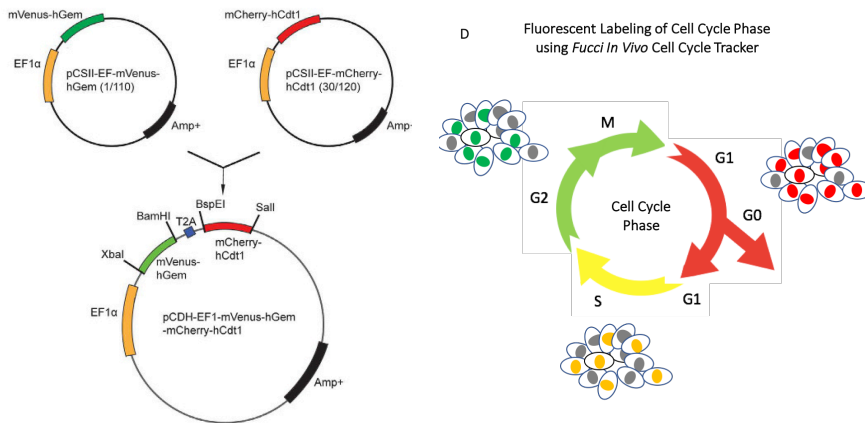
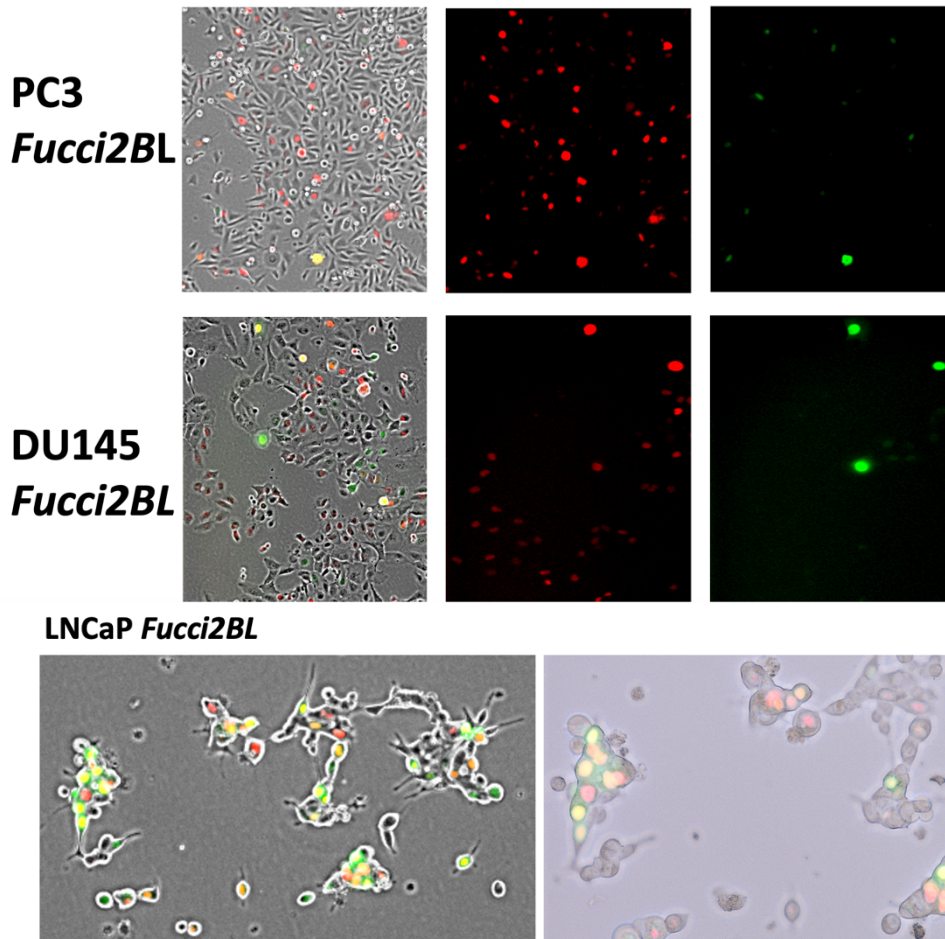


Fig 10. Fucci2BL vector generation and characterization. (a) Diagram and map of construct design and generation. Both mVenus-hGem(1/110) and mCherry-hCdt1 (30/120) were subcloned into a pCDHEF1 α -T2A lentiviral expression vector (b) Fluorescent labeling of cell cycle phases using Fucci2BL live cell cycle tracker system (Pineda *et al* 2016 Sci Rep).



6. **Identified a new dormant CRPC basal-luminal hybrid prostate cancer cell and gene signature under standard-of-care enzalutamide or androgen deprivation in PDX organoids** which may be targeted to eradicate dormant CRPC bone metastases in order to prevent disease recurrence. We will use this experimental paradigm of CRPC to test WNT5A and Cirmtuzumab in these organoids in combination with standard of care androgen deprivation therapy

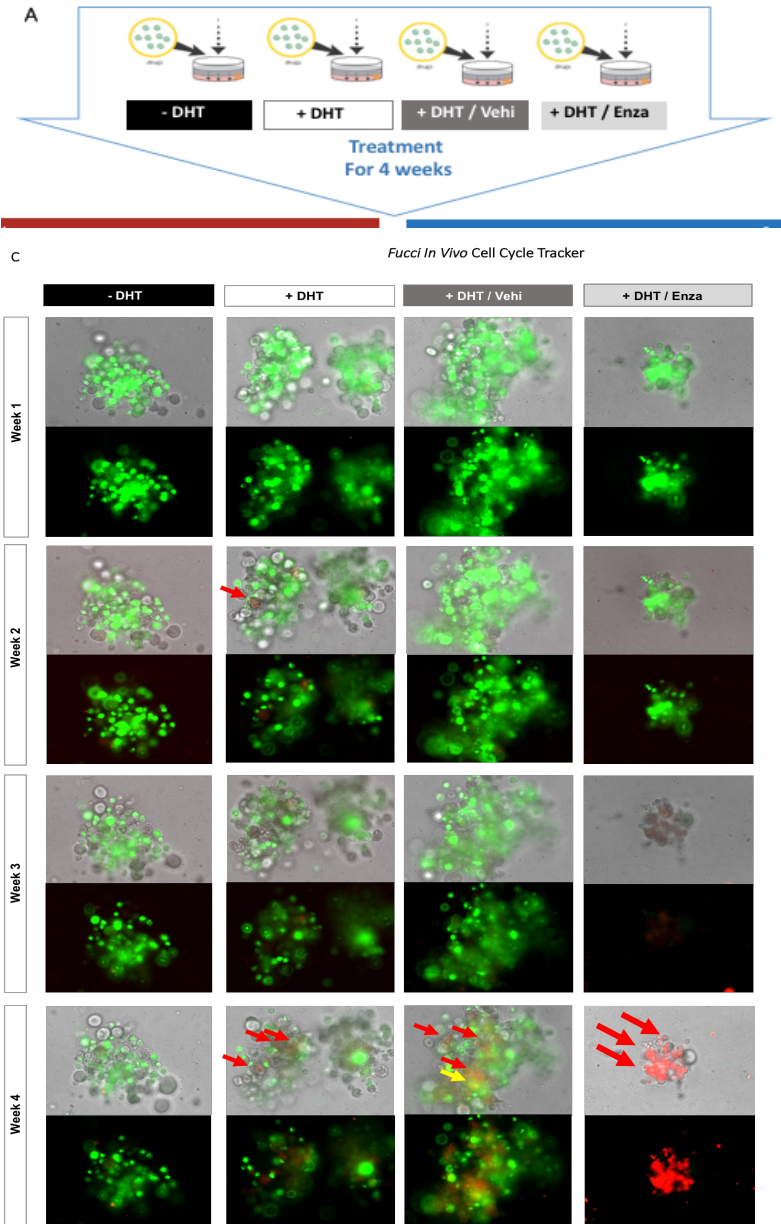


Figure 11. Enzalutamide-Resistant Population of PCSD1 Organoids are Dormant Cells.

Time course of cell cycle stages in live PCSD1 organoids under the four treatment conditions. Representative images in each treatment condition at week 1, 2, 3, and 4 of treatment of PCSD1 organoids stably expressing the *Fucci2 BL* bicistronic fluorescent, ubiquitination-based cell cycle indicator reporter system showing three cell cycle phases: G₁ / G₀ by red fluorescence, G₁/S by yellow fluorescence, and S/G₂/M by green fluorescence. The images of bright-field, red fluorescent channel and green fluorescent channel were taken and merged. (D) The *Fucci2 BL* fluorescent, ubiquitination-based cell cycle indicator reporter system visualizes the phase of cell cycle shown by colorimetric signal of red, yellow and green fluorescence for G₁, G₁/S and S/G₂/M, respectively.

Background: Androgen deprivation therapy (ADT) can help maintain remission in advanced prostate cancer (PCa) patients with bone metastases, however, growth and metastatic spread often recur.

Objective: To address the need for more predictive pre-clinical research platforms and to identify new targets and therapies for bone metastatic castration-resistant prostate cancer (CRPC).

Design, setting, and participants: We used patient-derived xenograft (PDX) tumors from bone metastatic prostate cancer patients to establish three-dimensional (3D) organoids and investigated their response to ADT by either withholding di-hydro-testosterone (no DHT) or treating with enzalutamide.

Outcome measurements and statistical analysis: Cyst/spheroid quantitation, immunohistopathology, cell viability assay, qRT-PCR, RNA sequencing, gene set enrichment analysis (GSEA) and live cell cycle tracking using *Fucci2BL* were performed.

Results and limitations: ADT resulted in CRPC spheroids with CK5⁺ CK8⁺ cells, up-regulated stem-cell transcription factors, steroidogenic and neurogenic pathways and down-regulated AR-target genes, interferon, cell cycle, cell division and circadian pacemaker pathways. Enzalutamide-treated spheroids transitioned to G₀ and AR protein was decreased but not AR mRNA. Moreover, ADT decreased both ACE2 and TMPRSS2, host cell viral entry factors for the severe acute respiratory syndrome (SARS) SARS-CoV-2.

Conclusions: This study identified a new dormant CRPC basal-luminal hybrid prostate cancer cell and gene signature which may be targeted to eradicate dormant CRPC bone metastases in order to prevent disease recurrence. The PDX organoids can be used also to screen for therapies that reduce ACE2 and TMPRSS2 expression thus suppressing viral load of SARS-CoV-2 and its variants.

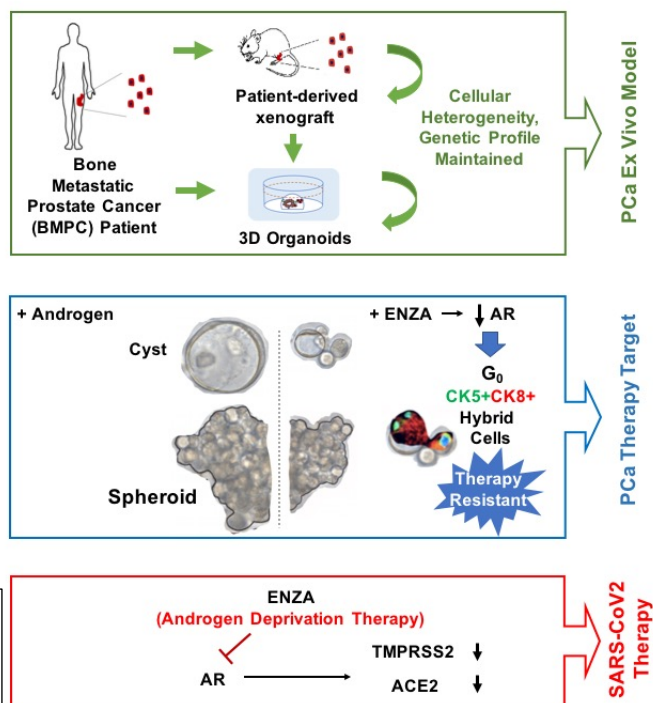
Patient Summary: In organoids, or **mini-tumors**, established from prostate cancer bone metastases, a novel type of dormant ADT-resistant cell with specific gene changes emerged which may be targeted to eradicate dormant metastases before they can progress. ADT also reduced the cell factors required for SARS-CoV-2 or its variants to infect its host cells and thus may reduce COVID-19 disease severity.

HIGHLIGHTS

- Patient-derived xenograft (PDX) models for bone metastatic prostate cancer and three-dimensional (3D) organoids (mini-tumors) more predictive pre-clinical research platforms.
- PDX Organoids used to test androgen deprivation therapy (ADT) resistance mechanisms.
- Novel hybrid basal-luminal cells that were ADT resistant, quiescent prostate stem-cell like gene expression profile.
- ADT decreased expression of the severe acute respiratory syndrome (SARS) SARS-CoV-2 host cell viral entry factors, TMPRSS2 and ACE2 as well as the Middle East respiratory syndrome (MERS) MERS-CoV receptor, DPP4 as well as anti-viral interferon response.
- Therefore, PDX organoids may be used to screen for novel therapies that target mechanisms of ADT resistance in PCa and for therapies that reduce TMPRSS2 and ACE2 expression and thus block SARS-CoV2 infection.

Figure 12. PDX organoids treated with Androgen deprivation therapy were CRPC and Dormant. Pre-clinical drug screening platforms for new CRPC and SARS-CoV2 and variants treatments.

GRAPHICAL ABSTRACT



7. Developing ROR1 CRISPR/Cas9 knock out in PCa cell lines and PDX PCSD13

The original plan was to knock down ROR1 using shRNA constructs. However, after discussions with Dr. Kipps lab members we decided to use CRISPR/Cas9 instead since shRNA does not sufficiently . We are using the Synthego Gene Knock Out Kit v2 – Human ROR1 along with the ThermoFischer Neon transfection system. We will perform and optimize CRISPR/Cas9 knock out in the PCa cell lines: PC3, DU145 and LNCaP. The PDX PCSD13 will be FACS sorted to enrich for ROR1 positive cells and then ROR1 will be knocked out with the Synthego CRISPR/Cas9 ROR1 kit.

8. Established ROR1 Immunohistochemical assay (IHC) for measuring ROR1 protein levels on pre-clinical studies in organoids, PDX models and in patient biopsies and tumor tissues.

Compared specificity and sensitivity of commercially available anti-ROR1 antibodies IHC staining was performed to determine optimal commercially available anti-ROR1 antibody such as 4A5 (Becton Dickinson) or ProteinTech, a rabbit polyclonal in the UCSD Tissue Technology Shared Resource histology core. IHC optimization was performed by Reveal Biosciences on control tissue formalin-fixed, paraffin-embedded (FFPE) tissue from a patient breast adenocarcinoma as shown in **Fig 13**. ProteinTech anti-ROR1 antibody showed highest specificity and sensitivity in optimization study.

We prepared control FFPE blocks of ROR1 positive control cell lines: Jeko, MCF7-ROR1, PC3, DU145 and negative control cell lines: RAJI, HS5 (WNT5A+) for IHC analysis. IHC analysis of Prostate cancer cell lines, PDXs, organoids and patient prostatectomy sections is currently underway.

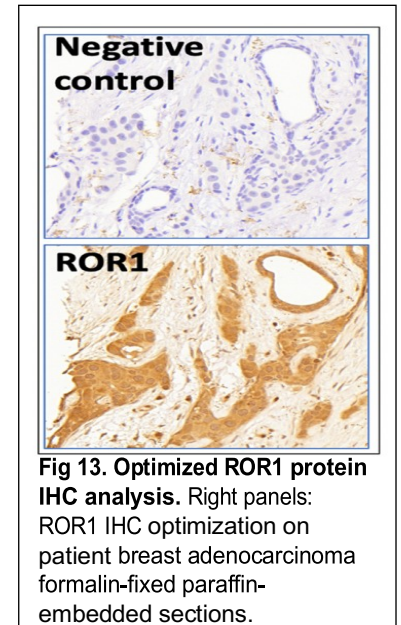


Fig 13. Optimized ROR1 protein IHC analysis. Right panels: ROR1 IHC optimization on patient breast adenocarcinoma formalin-fixed paraffin-embedded sections.

Specific Aim 2. Determine mechanism of action of ROR1-targeting antibody therapeutic, CIRMTUZUMAB (biologic), in pre-clinical trials using PDO and PDX models of bone metastatic prostate cancer. Perform IND-enabling studies and prepare for Phase 1B clinical trial for bone metastatic CRPC.

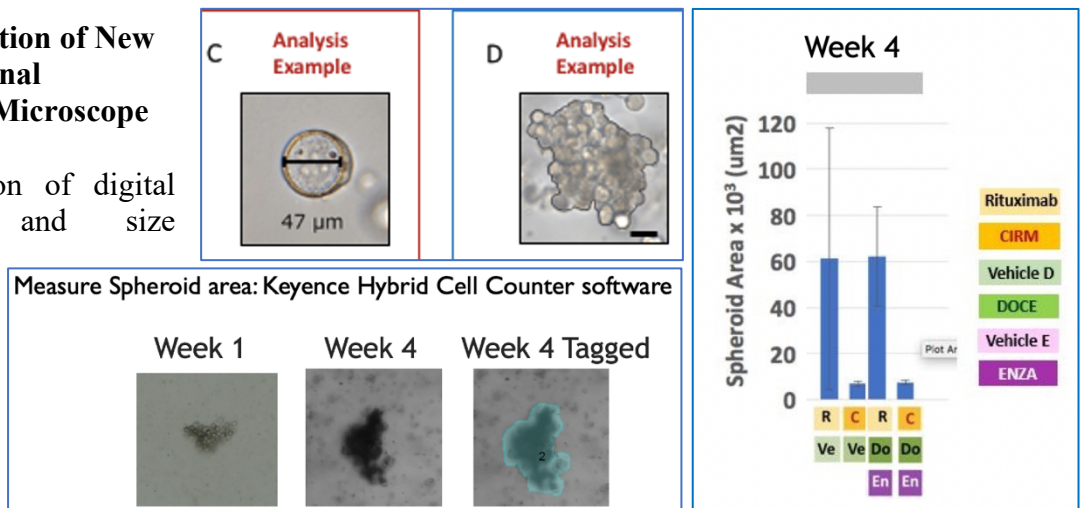
1. Characterizing docetaxel, cirmtuzumab response in PDX-derived organoids: PCSD1 and PCSD13

Performed quantitative analysis of the bone metastatic prostate cancer 3D organoids treated with combinations of the new cancer stem cell antibody therapeutic, Cirmtuzumab, plus standard of care therapies for metastatic prostate cancer: enzalutamide and docetaxel. We showed that Cirmtuzumab reduced the number and growth of the organoids (**Fig 14**). This is a critical result for the pre-clinical evidence supporting the IND-filing for FDA approval for the pending clinical trial of Cirmtuzumab in patients with metastatic prostate cancer.

Fig 14. Cyst and Spheroids in PCSD1 PDX organoids quantitation with Keyence Hybrid Count software. Cirmtuzumab reduced the number and growth of the spheroid organoids

2. Further Optimization of New Organoid Functional Response Digital Microscope Assay:

We improved quantitation of digital microscope number and size measurements of Cyst and Spheroid. This approach yields much more comprehensive understanding of the effects of treatments in live cells, over time than the standard viability end-point assays typically used in organoids. It is a key measurement to assess viability and growth in the PDX



organoids which are heterogeneous more like the disease in patients and contain two main types of multi-cellular masses: Cysts and Spheroids. These can respond differently to drug treatments as we have shown in our manuscript Lee et al, Appendix D. The cysts are more differentiated while the spheroids are less differentiated, more cancer stem-like and more therapy resistant. Evaluating them separately allows us to measure the effects on these different types of organoids in order to define the responsive and resistant tumor cells as seen reflected in heterogeneous responses of prostate tumors and metastases in patients.

We used the Keyence BZX710 digital microscope to capture images weekly and using the Keyence Hybrid count have measured the size and number of cysts and spheroids. This is an accurate but labor-intensive and time-consuming approach. Recently, we have worked with Reveal Biosciences, 6760 Top Gun St, Suite 100, San Diego, CA to develop more automated digital analysis software to analyze the large number of PDX organoid treatment experiments we have carried out. Analysis is underway for PCSD13 organoids treated with recombinant WNT5A protein plus Cirmtuzumab.

3. Performing *In vivo* PDX PCSD13 and ROR1+ PCa cell line xenograft experiments to test Cirmtuzumab +/- Docetaxel response and sequencing

a.) PDX pre-clinical trial for IND-filing for amendment for Phase clinical trial:

Group	Target Cells	Treatment (ROA)	N =
A	PCSD13 SC	Rituximab (control), vehicle	5
B		Rituximab + Docetaxel	5
C		Cirmtuzumab, vehicle	5
D		Cirmtuzumab + Docetaxel	5

b.) *In vivo* experiment using PC3-RFP-Luciferase plus Cirmtuzumab +/- Docetaxel: sub-cutaneous and intra-cardiac models. We have used the PC3-RFP-Luciferase cells we generated to test Cirmtuzumab-CART cells to inhibit sub-cutaneous tumor growth as shown below. We will use PC3-RFP-Luciferase cells to test efficacy of Cirmtuzumab plus Docetaxel as for PCSD13 described above. We will also perform intra-cardiac injection with PCR-RFP-Luciferase as a model of metastatic dissemination to test the ability of Cirmtuzumab to inhibit metastatic tumor growth. Mice will be monitored using *in vivo* bioluminescence (IVIS) as shown below for CART cell experiments.

Administrative Milestones:

- a. ACURO approval received
- b. HRPO: PDXs are exempt from HRPO in accordance with DoD Memo () and all samples from deceased subjects.

MILESTONES:

Specific Aim1: Determine the mechanism of WNT5A/ ROR1/ ROR2 signaling in bone metastatic CRPC using patient-derived organoids (PDO) and xenograft (PDX) models using shRNA and small molecule inhibitors of WNT-signaling.

1. ROR1 mRNA is expressed at high levels on castration resistant small cell PCa and neuroendocrine PCa (NEPC) cell lines and TCGA PCa dataset.
2. PCa cell lines, PC3 and DU145, express cell surface ROR1 protein
3. Generated PC3, DU145, LNCaP RFP-luciferase expressing cells for in vitro 2D and 3D growth and viability assays for testing Cirmtuzumab and WNT5A in vitro (Incucyte) and in vivo xenograft assays.
4. Established PC3 PCa cell line organoids (below, left) to study WNT5A:ROR1 signaling and Cirmtuzumab mechanism of action compared to PCSD1 (below, right) and PCSD13 PDX organoids.
5. Established Live Cell Cycle Tracking System – The Fucci2BL lentiviral vector for testing cell cycle changes in live organoids was established in PC3, DU145, LNCaP, PCSD1, PCSD13.
6. Identified a new dormant CRPC basal-luminal hybrid prostate cancer cell and gene signature under standard-of-care enzalutamide or androgen deprivation in PDX organoids which may be targeted to eradicate dormant CRPC bone metastases in order to prevent disease recurrence.
7. Developing ROR1 CRISPR/Cas9 knock out in PCa cell lines and PDX PCSD13
8. Established ROR1 Immunohistochemical assay (IHC) for measuring ROR1 protein levels on pre-clinical studies in organoids, PDX models and in patient biopsies and tumor tissues.

Specific Aim 2. Determine mechanism of action of ROR1-targeting antibody therapeutic, CIRMTUZUMAB (biologic), in pre-clinical trials using PDO and PDX models of bone metastatic prostate cancer. Perform IND-enabling studies and prepare for Phase 1B clinical trial for bone metastatic CRPC.

1. Characterizing docetaxel, cirmtuzumab response in PDX-derived organoids: PCSD1 and PCSD13
2. Further Optimization of New Organoid Functional Response Digital Microscope Assay.
3. Performing *In vivo* PDX PCSD13 and ROR1+ PCa cell line xenograft experiments to test Cirmtuzumab +/- Docetaxel response and sequencing

Administrative Milestones:

- c. ACURO approval received
- d. HRPO: PDXs are exempt from HRPO in accordance with DoD Memo () and all samples from deceased subjects.

4. IMPACT

Advanced prostate cancer is usually treated with Androgen deprivation therapy (ADT) which can help maintain remission in patients, however, growth and metastatic spread often recur. Treatments with new mechanisms of action are urgently needed. We are using patient-derived xenograft and PCa cell line models to test mechanism of action of a new therapeutic target: the WNT5A/ROR1 signaling pathway in prostate cancer for which a therapeutic ROR1 inhibitor antibody, Cirmtuzumab, has been developed and clinically tested in CLL and metastatic breast cancer patients. In Y1 of this grant we have shown that ROR1 is expressed at high levels on castration resistant small cell PCa and neuroendocrine PCa (NEPC) models; two of the most lethal forms of prostate cancer for which there are no curative treatments in PCa cell lines and PDX models. Cirmtuzumab has demonstrated efficacy in our patient derived xenograft organoid cultures. We are now performing in vitro and in vivo testing in NEPC cell lines and in our patient-derived xenograft (PDX) mouse models. We have developed immunohistochemistry (IHC) assays to detect ROR1 in patient biopsy samples which will allow us to define the prostate cancer patient population that expressed ROR1 and to be able to evaluate the treatment in patients for a future clinical trial. These studies are will inform us about the appropriate patient populations for treatment and clinical trials. These pre-clinical studies being performed in this grant will support the pending Phase 1B clinical trial (not part of this grant).

IRB-approved clinical trial:

Co-Investigator, A Phase 1B, Nonrandomized Trial Investigating Docetaxel Combined with Cirmtuzumab in Patients with Metastatic Castration Resistant Prostate Cancer. **PI: Dr. J. Kellog Parsons, UCSD, Co-Investigator: Dr. Rana Mckay.**

We are performing the pre-clinical studies required for filing for an amendment to IND approval at the FDA to perform the clinical trial in prostate cancer patients. I will be guiding the analysis of the Cirmtuzumab target, ROR1, IHC assays on biopsies from patient metastases on the trial to assess the effectiveness of Cirmtuzumab therapy. In parallel we will be performing ROR1 IHC analysis in a cohort of archived pathology patient biopsy and prostatectomy specimens to further define the prostate cancer patients who may benefit from this therapy.

5. CHANGES/PROBLEMS

1. Special Comments about COVID-19

The COVID-19 pandemic threw all of us into survival mode and required us to adapt to a new way to work to ensure the safety and continued productivity of our teams. This gave us all the opportunity to reset and creatively renew our work and assumptions about our lives. I have successfully pivoted my efforts and those of my team to maintain progress and exponentially increase skills, and most notably, our adaptability to our new COVID-19 work-style and our ability and motivation to get work done.

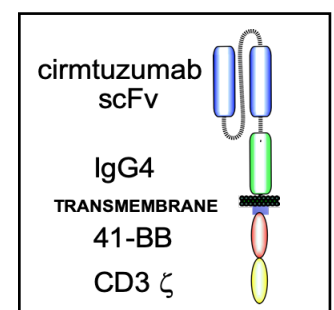
With the lab shut down from March 18th, 2020 to June 30th, 2020 my team and I shifted our efforts to our bioinformatics and digital microscope image analyses which we could do remotely. I upgraded our computer and software for everyone on our team and we were able to work efficiently as a team remotely. I had daily calls with my lab manager and postdoctoral fellow, weekly lab meetings of the whole team and weekly meetings with the undergraduate researchers and Visiting Scholar. We have several experiments already performed for which several hundred images remain to be analyzed. We have also reached out to a local company, Reveal Biosciences, to help our team with independent data analysts.

My lab manager and postdoctoral fellow maintained our irreplaceable patient samples and models. Now that we are allowed 25% lab occupancy time, we are doing new experiments with these models. These pre-clinical experiments are also being used for IND-filing for FDA approval of a new clinical trial for Cirmtuzumab in advanced prostate cancer patients.

We increased our bioinformatics efforts and are performing RNA sequencing of RNA from the organoid and PDX experiments. In collaboration with our bioinformatician, Dr. Terry Gaasterland, PhD, Professor of Computational Genetics, UCSD, we are performing gene expression profiling to identify gene signatures altered by WNT5A and Cirmtuzumab treatment. My undergrads and new graduate student are learning to use publicly available bioinformatics software: Genesis and GSEA to perform directed analysis of gene signatures identified in previous studies of prostate cancer stem cells and Cirmtuzumab treated patients from different cancers. They are reviewing the literature to compile the gene lists and use these to query the RNA sequencing data sets from our organoid experiments. This will help to identify the key genes and signaling pathways that may be used as biomarkers for monitoring effectiveness of Cirmtuzumab in patients in the clinical trial and for designing combination treatment plans with appropriate standard of care regimens.

2. **Recently**, we tested Chimeric antigen receptor (**CAR**)-T cells made with the Cirmtuzumab antibody and have shown that these CART cells completely kill ROR1 expressing PCa cell lines and PDX cells in culture. The Cirmtuzumab-based CAR-T cells can kill cells in culture that are from two of the most lethal types of prostate cancer: castration resistant PCa (CRPC) and NEPC. We are testing these our mouse xenograft in vivo and hope to use these CART cells to see if we can eradicate lethal prostate cancers in a clinical trial. CART cells are killer T cells engineered with a chimeric receptor that combines the known specificity of an antibody with the signaling activator that engages the killing machinery of the T cell. Therefore, the engineered killer T cell can be directed toward a desired target on a cell such as a prostate cancer cell. CART cells are a way to direct the awesome power of the immune system that can truly eradicate cancer as shown in some melanomas and leukemias. We hope to use CART cells that target ROR1 to eradicate two of the most lethal forms of prostate cancer: CRPC and NEPC.

Fig 1 ROR1 targeting Cirmtuzumab based Chimeric Antigen Receptor (CAR) T cell.



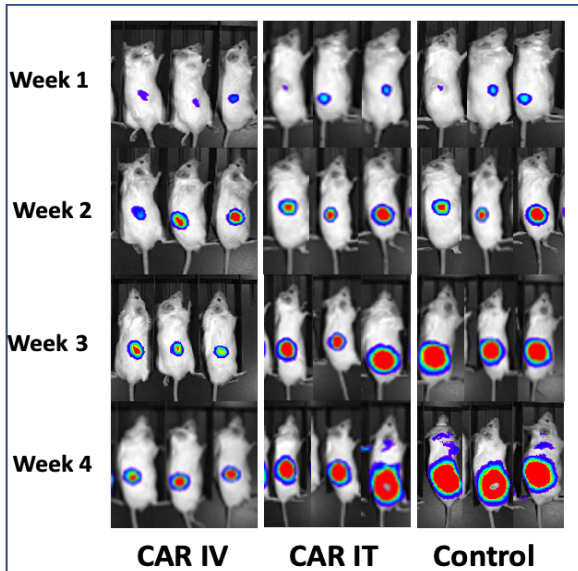


Figure 11-Bioluminescence imaging of mice implanted subcutaneously with PC3 PCa cells and Treated with ROR1 CAR T-cells. Animals were implanted with 2e6 luciferase expressing PC3 cells on day 1 and were treated with the one-time injection of 3e7 CAR-T cells IV (**CAR IV**) or activated mock transduced cell (**Control**) or 1e7 cells administered intra-tumorly (**CAR IT**) As shown, the CAR-T treated mice that received a single intravenous or intra-tumoral injection had reduced disease burden when compared to control animals, which had to be sacrificed by week 5 The CAR-T IV treated cohort had only minimal amounts of disease at the end of the study, which validates the use of this model for the planned studies detailed in this proposal.

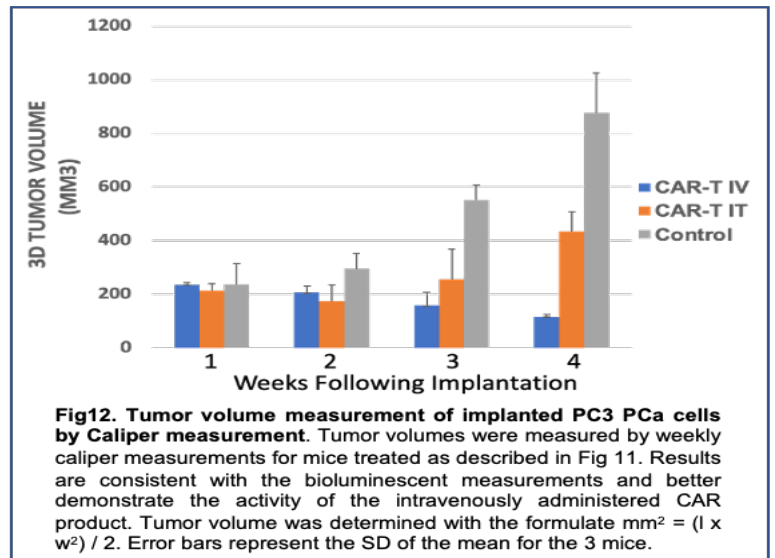


Fig12. Tumor volume measurement of implanted PC3 PCa cells by Caliper measurement. Tumor volumes were measured by weekly caliper measurements for mice treated as described in Fig 11. Results are consistent with the bioluminescent measurements and better demonstrate the activity of the intravenously administered CAR product. Tumor volume was determined with the formulate $\text{mm}^3 = (l \times w^2) / 2$. Error bars represent the SD of the mean for the 3 mice.

10. Products

Cirmtuzumab (Oncternal, Inc) therapeutic antibody

To date, no Wnt signaling inhibitors, including ROR1 targeting agents, have been approved for clinical use in the treatment of cancer. Because it has been shown to be expressed on a number of highly malignant hematological and solid tumor cancers, including CRPC and NEPC cells from patient derived samples and has a demonstrated functional role in oncogenesis, ROR1 is an attractive therapeutic target (Table 1). To target this proto-oncogene, cirmtuzumab, a first-in-class ROR1 binding monoclonal antibody (mAb) was developed at the University of California San Diego (UCSD) by Drs. Thomas Kipps, and Charles Prussak with funding support from the California Institute for Regenerative Medicine (45). This humanized mAb has a high affinity for human ROR1 and no apparent off-target activities in in vitro or in vivo test systems.

Based on a battery of preclinical studies, a pilot phase I study of single agent cirmtuzumab was conducted in patients with relapsed/refractory chronic lymphocytic leukemia. In this clinical study, the anti-ROR1 mAb was well tolerated with no antibody associated serious adverse events noted, had a prolonged half-life no off-tumor normal tissue binding and early evidence of anti-tumor activity (NCT02222688) (44).

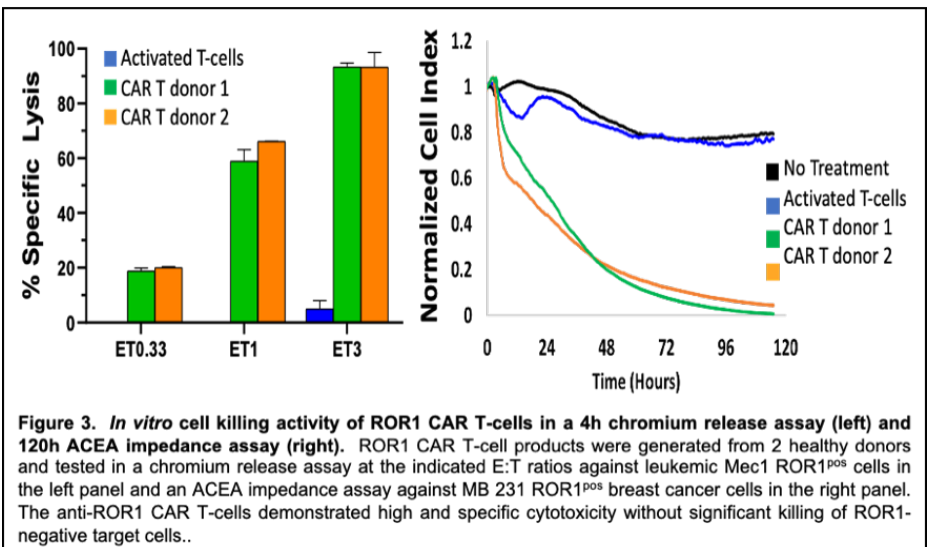
Cancer Type	ROR1 Expression (%)
Uterus	96
MCL	>95
CLL	95
Lymphoma	90
Prostate	90
Skin	89
Pancreas	83
Adrenal	83
Lung	77
Breast	75
Testicular	73
Colon	57
Ovarian	54
Bladder	43

Table 1. Cancer type and percentage of ROR1 expression

Because of its favorable therapeutic index, cirmtuzumab has subsequently been studied in a number of clinical trials targeting lymphoid and solid tumor cancers in combination with standard chemotherapies (NCT02776917, 02860676 and 03088878), as the targeting moiety for an antibody drug conjugate (ADC) (NCT03833180) and an IRB-approved Phase 1b clinical trial with this mAb is imminent for patients with metastatic CRPC.

For these reasons, solid tumor cancers of the breast, prostate, lung and colon represent particularly intriguing targets for anti-ROR1 targeting therapies with elevated expression of this proto-oncogene being detected on more malignant forms of these cancers. For example, we have demonstrated elevated expression of ROR1 on highly malignant, taxane resistant, breast cancer cells (Table 1). Because this mAb blocks ROR1 signaling by blocking Wnt5A mediated activation, cirmtuzumab has demonstrated substantial therapeutic activity against these chemotherapy resistant tumors in preclinical models. Based on these studies, a phase 1b clinical trial combining cirmtuzumab with paclitaxel

is being tested in patients with advanced breast cancer (NCT02776917)(34). Like breast cancer, a taxane (docetaxel) based chemotherapy regimen is a mainstay for the treatment of patients with advanced CRPC(72). However, when combined with abiraterone and enzalutamide, this docetaxel containing chemotherapy cocktail has minimal activity in treating CPRC, generating a 3- month median time to progression and limited impact on reducing PSA levels (<30% of patients) (73). Additionally, noncanonical Wnt signaling has been hypothesized to be a mechanism of resistance to enzalutamide(28) and taxane chemotherapy (63). Available data suggest that Wnt blockade with chemotherapy may be the most effective way to implement Wnt pathway modulation(52).



11. Participants & Other Collaborating Organizations

Co-investigators:

Dr. Terry Gaasterland, PhD, Professor of Computational Genetics, UCSD, we are performing gene expression profiling to identify gene signatures altered by WNT5A, ROR1 CRISPR/Cas9 knock out, and Cirmtuzumab treatment alone, with standard-of-care: enzalutamide +/- docetaxel, or in combination in PDX organoids and PDX in vivo. Performed expression profiling and GSEA analysis in PDX organoids plus ADT for Lee, Mendoza, Burner et al (manuscript Submitted to European Urology, attached as Appendix D).

Dr. Nicholas A. Cacalano, PhD, Associate Professor, Dept of Radiation Oncology, UCLA, is performing the CRISPR/Cas9 KO, performing ROR1 IHC and IFC on PCa cell lines and PDX Fucci2BL expressing organoids and working on ROR1 expression analysis and western optimization for PCa cell lines, organoids and PDXs.

Dr. Karl Willert, PhD, Associate Professor, Dept of Medicine, UCSD, has provided WNT5A recombinant protein and the Porcupine inhibitor for in vitro assays in PDX and PCa cell line models. Discussions and experiment planning and interpretation.

Dr. Rana McKay, MD, Associate Professor, Dept of Medicine, UCSD, GU Oncologist, and

Dr. Christopher Kane, MD, Professor, Dept of Urology, UCSD

Cirmtuzumab clinical trial planning and discussion of pre-clinical in vivo trial design to support and inform IND-enabling FDA approval of Phase 1B Clinical trial planning with UCSD Alpha Stem Cell Clinic, identification of target population, wrote and submitted IRB protocol which has been approved.

Co-Investigator, A Phase 1B, Nonrandomized Trial Investigating Docetaxel Combined with Cirmtuzumab in Patients with Metastatic Castration Resistant Prostate Cancer. PI: Dr. J. Kellog Parsons, UCSD, Co-Investigator: Dr. Rana McKay.

12. Special Reporting Requirements

N/A

13. Appendices

A. OPR Memo on PDX and HRPO

B. Technical Abstract

C. SOW

D. Manuscript: Lee, Mendoza, Burner et al. (pdf Attached)



DEPARTMENT OF THE ARMY
HEADQUARTERS, U.S. ARMY MEDICAL RESEARCH AND DEVELOPMENT COMMAND
810 SCHREIDER STREET
FORT DETRICK, MARYLAND 21702-5000

FCMR-RP

MEMORANDUM FOR RECORD

SUBJECT: Clarification of Office of Research Protections (ORP) oversight of the use of existing, established PDX models in USAMRDC supported research.

1. References:

a. Memorandum, SECARMY, 5 November 2019, subject: Army Policy for Use of Human Cadavers for Research, Development, Test and Evaluation, Education or Training.

b. Guidance on HRPO Review Requirements for Research Involving the Secondary Use of Data/Specimens, 8 May 2020

2. This memorandum serves to clarify that USAMRDC supported research involving the use of established, existing patient derived xenograft (PDX) models (or the cell lines derived therein) that were established using tissue from deceased donors does not require ORP Human Research Protection Office's review and oversight for cadaver use in accordance with reference (a).

3. HRPO submission and review remains required when DoD funding is used to combine human specimens (e.g. cell lines, tissue) with non-human material to create a xenograft for research use in accordance with reference (b). In addition, the use of established, existing PDX models established using tissue from living donors and/or the creation of cell lines from established, existing PDX models currently does not require MRDC HRPO review.

4. The research use of established, existing PDX models created without DoD support (e.g., research with mice) does require institutional animal use and USAMRDC ORP Animal Care and Use Review Office (ACURO) review.

Kimberly L. Odam, MS,CIP
Director
Office of Research Protections

Technical Abstract: Targeting WNT5A-mediated Therapy Resistance Mechanisms and Tumor Genomic Heterogeneity in Lethal Bone Metastatic Prostate Cancer.

BACKGROUND: One in six men will be diagnosed with prostate cancer (PCa), making it one of the leading health problems affecting men in today's society. Patients diagnosed during the earlier stages are surviving longer due to improved therapies. However, a growing number of these patients later go on to develop advanced PCa. Since the 2012 USPSTF recommendation against PSA screening there has also been an increase in the number of men presenting with higher grade, metastatic prostate cancer. The main treatment for advanced prostate cancer (PCa) is androgen deprivation therapy (ADT) which targets androgen receptor (AR) signaling. Unfortunately, patients invariably become resistant to ADT, that is, they develop castrate resistant prostate cancer (CRPC) and their cancer metastasizes - most often to bone.

Bone metastatic prostate cancer affects the majority of men with advanced prostate cancer and is present in more than 90% of patients who die of the disease. Bone metastases cause extreme pain and some of the most debilitating effects of cancer in patients including pathologic fractures and spinal compression that require significant and ongoing intervention. It is also associated with increased therapy resistance and lethal, malignant disease progression. There are no curative treatments for bone metastatic prostate cancer. Therefore, development of therapies that increase therapeutic targeting of PCa in the bone is urgently needed.

RATIONALE: Prostate cancer (PCa) is highly heterogeneous making it difficult to treat with targeted therapies. Most bone metastatic PCa develops therapy resistance. We and others showed WNT5A, a Wnt-family ligand, is correlated with bone metastatic, castrate resistant PCa (bmCRPC). Here, we aim to determine the involvement of WNT5A in ADT therapy resistance and to test CIRMTUZUMAB, the WNT5A receptor, ROR1-inhibiting antibody biologic therapy, for its effectiveness against bmCRPC in pre-clinical, IND-enabling studies leading to a Phase 1B clinical trial. Next, we will define the gene expression profiles at the single cell level of ADT therapy resistant metastatic cells in a biobanked series of surgical prostate cancer bone metastasis specimens and matched PDO and PDX models. Single cell RNASeq gene expression profiles will allow us to measure heterogeneity of the patient tumor cells and the non-tumor cells of the bone microenvironment in our collection of twenty surgical patient prostate cancer bone metastasis samples and patient-derived xenografts. Single cell RNA sequencing is best performed using viable, single cells. To the best of our knowledge we are the only group to have a biobank of these rare patient samples cryopreserved as viable, single cells.

HYPOTHESIS: WNT5A and its downstream signaling pathways were strongly up-regulated in the bone-niche in our patient specimens and in their matched xenografts (PDX). We postulate that WNT5A/ROR1/ROR2 signaling supports early stage, androgen-independent prostate development which may be re-accessed in bone metastatic prostate cancer under the selection pressure imposed by anti-androgen treatment. Our model states that anti-androgen suppression of AR may induce the expression of WNT5A and subsequently a prostate stem/progenitor cell-like program that mimics early prostate development in low or no androgen conditions. We propose experiments to test our hypothesis that inhibition of WNT5A expression and/or signaling via blocking its receptor, ROR1, will eradicate the tumor initiating and tumor perpetuating cells in the bone niche.

AIM 1. Determine the mechanism of WNT5A/ ROR1/ ROR2 signaling in bone metastatic CRPC using patient-derived organoids (PDO) and xenograft (PDX) models using shRNA and small molecule inhibitors of WNT-signaling. **AIM 2.** Determine mechanism of action of ROR1-targeting antibody therapeutic, **CIRMTUZUMAB** (biologic), in pre-clinical trials using PDO and PDX models of bone metastatic prostate cancer. Perform IND-enabling studies and prepare for Phase 1B clinical trial for bone metastatic CRPC. Cirmtuzumab is in Phase 1b clinical trials for CLL and metastatic breast cancer. **AIM 3.** Perform single cell RNASeq analysis on our unique series of surgical patient prostate cancer bone metastasis specimens. Determine single cell RNA profiles of tumor and bone environment non-tumor cells in our biobank of twenty viably cryopreserved, surgical patient prostate cancer bone metastases and the organoids and xenografts derived from them. We have used these PDO and PDX models to test standard of care therapies for inhibiting prostate cancer growth. Thus, we are poised to use our PDX and PDO models to test novel WNT5A targeting therapies to overcome bone-niche mediated CRPC. The proposed research addresses two of the PCRP 2018 overarching challenges: 1. to develop treatments that improve outcomes for men with lethal prostate cancer and 2. to define the biology of lethal prostate cancer to reduce death.

STATEMENT OF WORK – 10/10/2018
PROPOSED START DATE Oct 01, 2019

Site 1: Moores Cancer Center,
UC, San Diego (UCSD)
3855 Health Sciences Drive
La Jolla, CA 92093820
PI: Dr. Christina Jamieson

Site 2: Dept of Radiation Oncology,
UC, Los Angeles (UCLA)
10833 LeConte Ave.,
Los Angeles, CA 9
PI: Dr. Nicholas A. Cacalano

SPECIFIC AIMS	Timeline	Site 1	Site 2
Specific Aim 1: Determine mechanism of WNT5A signaling in bone metastatic CRPC using PDX and PDO models.			
Major Task 1: Gene silencing (shRNA) of WNT5A, ROR1 and ROR2 in patient-derived xenograft (PDX) models.			
Subtask 1: WNT5A, ROR1 and ROR2 will be silenced in 3 PDXs: PCSD1, PCSD5 and PCSD13 using commercially available shRNA lentiviral particles.	1-6 months	CJ	
Subtask 2: Confirm WNT5A, ROR1, ROR2 silencing in xenografts: Immunoblotting.	3-7	KW	NC
Major Task 2: Determine effect of silencing WNT5A, ROR1 or ROR2 on tumor growth and signaling <i>in vivo</i> .			
Subtask 3: Expt. 1. <u>Intra-femoral</u> injection of <u>PCSD1 shRNA</u> control, shRNA_WNT5A, shRNA_ROR1 and shRNA_ROR2. Establish intra-femoral xenografts in 40 male <i>Rag2^{-/-}γc^{-/-}</i> , n=10 mice x 4 shRNA stably transduced lines. Measure tumor growth using calipers and IVIS, serum PSA and ALP. Harvest at 8 weeks or max tumor size for qPCR, RNASeq and immunoblotting of WNT5A, ROR1, ROR2 and signaling pathways. MicroCT of bone lesions, IHC, IFC PCa markers.	3-6	CJ KW TG	NC
Subtask 4: Expt. 2. <u>Intra-femoral</u> injection <u>PCSD5 shRNA</u> control, shRNA_WNT5A, shRNA_ROR1 and shRNA_ROR2. Establish bone metastatic intra-femoral PCa in 40 male <i>Rag2^{-/-}γc^{-/-}</i> mice. Measure tumor growth and collect tumor tissues as above.	6-10	CJ KW TG	NC
Subtask 5: Expt. 3. <u>Intra-femoral</u> injection <u>PCSD13 shRNA</u> control, shRNA_WNT5A, shRNA_ROR1 and shRNA_ROR2. Establish bone metastatic intra-femoral PCa in 40 male <i>Rag2^{-/-}γc^{-/-}</i> mice. Measure tumor growth and collect tumor tissues as above.	9-12	CJ KW TG	NC
Subtask 6: Expt. 4. <u>Intra-cardiac</u> injection of PCSD1, PCSD5 and PCSD13 with shRNA control, shRNA_WNT5A, shRNA_ROR1 and shRNA_ROR2 into 5 male <i>Rag2^{-/-}γc^{-/-}</i> mice per shRNA, Total = 60 mice. Measure #, size metastases using IVIS.	12-15	CJ KW TG	NC
Subtask 7: Expt. 5. <u>Intra-femoral</u> <u>PCSD1 shRNA_ROR1 plus ENZALUTAMIDE</u> (ADT). Establish bone metastatic intra-femoral PCa in 40 male <i>Rag2^{-/-}γc^{-/-}</i> mice. Treat with vehicle or enzalutamide daily, 28 days. Measure tumor growth using calipers and IVIS, Serum for PSA, ALP. Collect tumor tissue at end of treatment for qPCR, RNASeq and immunoblotting of PCa markers and WNT5A/ROR1/ROR2 signaling. MicroCT analysis of bone lesions and IHC, IFC of PCa markers.	16-19	CJ KW TG	NC
Subtask 8: Expt. 6. <u>Intra-femoral</u> <u>PCSD5 shRNA_ROR1 plus ENZA</u> (ADT). Establish intra-femoral PCa in 40 male <i>Rag2^{-/-}γc^{-/-}</i> mice. Treat and analyze as above.	20-23	CJ	
Subtask 9: Expt 7. <u>Intra-femoral</u> <u>PCSD13 shRNA_ROR1 plus ENZA</u> (ADT). Establish intra-femoral PCa in 40 male <i>Rag2^{-/-}γc^{-/-}</i> mice. Treat and analyze as above.	24-27	CJ KW	NC
Subtask 10: Bioinformatics on all RNASeq, qPCR and immunoblotting confirmation	28-34	CJ TG	NC

Milestone #1: Manuscript on WNT5A, ROR1, ROR2 signaling and role in ADT resistance in bone metastatic PCa.	32-36	CJ KW TG	NC
Major Task 3: Define proteins interacting with ROR1 in PDX intra-femoral tumors using Mass Spectrometry.			
Harvest tumors from mice with PCSD1, PCSD5 and PCSD13 intra-femoral xenografts. Extract protein from fresh tumor tissue, immunoprecipitate with anti-ROR1 or isotype control antibody. Analyze by Mass Spec to identify co-immunoprecipitating proteins.	1-2	CJ	NC
Confirmation of protein-protein interactions by co-ip and immunoblotting for ROR1.	3-9		NC
Milestone #2: Manuscript ROR1-associating proteins in patient derived bone met PCa.	9-18	CJ	NC
Major Task 4: Determine effect of silencing WNT5A, ROR1 or ROR2 on viability, growth and signaling <i>in vitro</i> using 3D/ patient derived organoid (PDO) models of bone metastatic prostate cancer.			
Establish 3D/organoid cultures from PCSD1, PCSD5 and PCSD13 cells with shRNAcontrol, shRNA_WNT5A, shRNA_ROR1 and shRNA_ROR2.	6-8	CJ	
Treat with vehicle or enzalutamide for 4 weeks then measure viability, cysts, spheroids, PSA (IHC), apoptosis (Cleaved caspase 3 IFC), proliferation (Ki67), Basal cells: CK5, p63, Luminal cells: CK8, FZD, RTK signaling mediators by IFC, confocal microscopy.	6-12	CJ KW	NC
Milestone #3: Manuscript on mechanism of WNT5A signaling in 3 PDOs of bone met PCa.			
Specific Aim 2: Determine mechanism of action (MOA) of ROR1-targeting biologic, CIRMTUZUMAB in PDO and PDX models of bone metastatic PCa.			
Major Task 1: Use PDOs from PCSD1, PCSD5 and PCSD13 to test Cirmtuzumab alone or in combination with standard of care therapies.			
Subtask 1: <u>PCSD1 in 3D/organoid</u> culture plus Cirmtuzumab +/- Enza, +/- docetaxel, +/-irradiation (IR), +/-olaparib, + IR+olaparib, + PORCN inhibitors:. Measure overall viability, size and number of cysts and spheroids, PSA, apoptosis (Cleaved caspase 3), proliferation (Ki67), Basal cells: CK5, p63, Luminal cells: CK8, FZD, RTK signaling.	1-6	CJ KW	NC
Subtask 2: <u>PCSD5 in 3D/organoid</u> culture plus Cirmtuzumab alone, or in combination with enzalutamide, docetaxel, IR, olaparib, IR plus olaparib, PORCN inhibitors.	1-6	CJ KW	NC
Subtask 3: <u>PCSD13 in 3D/organoid</u> culture plus Cirmtuzumab alone, or in combination with enza, docetaxel, IR, olaparib, IR plus olaparib, PORCN inhibitors.	1-6	CJ KW	NC
Major Task 2: Use PDXs from PCSD1, PCSD5 and PCSD13 to test Cirmtuzumab <i>in vivo</i> with enzalutamide.			
Subtask 1: Expt. 1. <u>PCSD1-GFP Luciferase</u> Establish bone metastatic intra-femoral xenografts with PCSD1 in 40 male <i>Rag2^{-/-}γc^{-/-}</i> , n=10 mice x 4 groups: 1. Vehicle, isotype Ab control/ 2. Enza, isotype Ab control / 3. Vehicle, CIRM/ 4. Enza, CIRM. Measure tumor growth: calipers, IVIS, Serum PSA,ALP. Tumor: qPCR, RNASeq and immunoblotting: WNT5A, ROR1, ROR2 signaling pathways. MicroCT, IFC, IHC.	6-12	CJ, KW TG	NC
Subtask 2: Expt. 2. <u>PCSD5-GFP Luciferase</u> Establish bone metastatic intra-femoral xenografts with PCSD1 in 40 male <i>Rag2^{-/-}γc^{-/-}</i> , n=10 mice x 4 groups. Treat and analyze as above.	12-18	CJ, KW TG	NC
Subtask 3: Expt. 3. <u>PCSD13-GFP Luciferase</u> Establish bone metastatic intra-femoral xenografts with PCSD1 in 40 male <i>Rag2^{-/-}γc^{-/-}</i> , n=40 mice. Treat and analyze as above.	18-24	CJ KW TG	NC
Milestone #4: Manuscript on efficacy of CIRMTUZUMAB in PDX and PDO models of bone metastatic PCa.	24-28	CJ KW TG	NC

Major Task 3: Prepare for Clinical trial for CIRMTUZUMAB in bone metastatic CRPC			
Phase 1B Clinical trial planning with UCSD Alpha Stem Cell Clinic, identification of target population, writing and submitting IRB protocol. Informed by ongoing clinical trials in CLL and breast cancer.	12-36	CJ CK RM	
Prepare regulatory documents to obtain CIRMTUZUMAB for clinical trial	12-36	CJ PW	
<i>Milestone #5: IRB approved clinical trial protocol and CIRMTUZUMAB supply for trial.</i>			
Specific Aim 3: Determine single cell RNA profiles and deep RNASeq whole transcriptome profiling of sorted tumor cells and microenvironment cells of patient surgical bone metastasis samples.			
Purify viable, single cells from cryopreserved patient bone metastasis samples PCSD1-PCSD20, and normal bone marrow then immediately transport to Dr. Kristen Jepsen, UCSD IGM for 10XGenomics platform sample preparation and single cell RNA sequencing.	24-28	CJ	
Bioinformatics to identify different cell types from expression profiles and to identify tumor cell specific surface markers for sorting tumor cells from microenvironment cells, eg. PSMA	28-30	TG	
FACS sort tumor cells from microenvironment cells and make RNA, Deep RNASeq of RNA from sorted bone metastatic tumor cells, microenvironment cells and normal bone marrow.	30-33	CJ TG	
Bioinformatic analysis of Deep RNASeq of patient bone met samples and all PDX experiments.	33-36	CJ TG	
<i>Milestone #6: Manuscript of single cell RNA and whole transcriptomic analysis of patient bone metastatic prostate cancer samples and xenografts to distinguish tumor and bone microenvironment profiles for biomarker and prognostic signatures of bone marrow fine needle aspirate/biopsies of bone metastases.</i>			

1 **Title Page**

2

3 **Dormant castration-resistant prostate cancer organoids**
4 **with hybrid basal-luminal cells and loss of SARS-CoV-2 host factors**
5 **emerge under androgen deprivation**
6

7

8 Sanghee Lee^{1,2,3}, Theresa R. Mendoza^{1,2,3}, Danielle N. Burner^{1,2,3}, Michelle T. Muldong^{2,3}, Christina
9 N. Wu^{3,4}, Catalina Arreola^{2,3}, Abril Zuniga^{2,3}, Olga Miakicheva-Greenburg^{2,3}, William Y. Zhu^{2,3}, Gabriel
10 Pineda⁴, Kathleen M. Lennon⁴, Nicholas A. Cacalano⁵, Catriona H.M. Jamieson⁴, Christopher J.
11 Kane^{2,3}, Anna A. Kulidjian⁶, Terry Gaasterland⁷, and Christina A.M. Jamieson^{2,3,8,*}

12

13 ¹These authors contributed equally.

14 ²Department of Urology, University of California, San Diego, La Jolla, California, 92093, USA

15 ³Moore's Cancer Center, University of California, San Diego, La Jolla, California, 92093, USA

16 ⁴Department of Medicine, University of California, San Diego, La Jolla, California, 92093, USA

17 ⁵Department of Radiation Oncology, University of California, Los Angeles, Los Angeles, California,
18 90095, USA

19 ⁶Scripps MD Anderson Cancer Center, La Jolla, California, 92093, USA

20 ⁷ Scripps Institute of Oceanography, University of California San Diego, La Jolla, California, 92093,
21 USA

22

23 ⁸Lead contact

24 *Corresponding author: Christina A.M. Jamieson, University of California San Diego, 4326 Moore's
25 Cancer Center, 3855 Health Science Drive, La Jolla California, United States, 92093-0820, Tel. 1-
26 858-534-2921, Fax. 858-822-6288. e-mail: camjamieson@health.ucsd.edu (C.A.M.J)

27

28

29

30 **Keywords**

31 Androgen Deprivation Therapy, Angiotensin-Converting Enzyme 2 (ACE2), Basal-luminal hybrid,
32 Bone Metastatic Prostate Cancer, Enzalutamide, Patient-derived Organoids, Patient-Derived
33 Xenograft (PDX), SARS-CoV-2, Transmembrane Protease Serine 2 (TMPRSS2)

34
35 **Word count of the text**

36 **Word count of the abstract** 300

37
38 **Abstract (Final Version: 300, updated by CJ)**

39
40 **Background:** Androgen deprivation therapy (ADT) can help maintain remission in advanced prostate
41 cancer (PCa) patients with bone metastases, however, growth and metastatic spread often recur.

42 **Objective:** To address the need for more predictive pre-clinical research platforms and to identify new
43 targets and therapies for bone metastatic castration-resistant prostate cancer (CRPC).

44 **Design, setting, and participants:** We used patient-derived xenograft (PDX) tumors from bone
45 metastatic prostate cancer patients to establish three-dimensional (3D) organoids and investigated
46 their response to ADT by either withholding di-hydro-testosterone (no DHT) or treating with
47 enzalutamide.

48 **Outcome measurements and statistical analysis:** Cyst/spheroid quantitation,
49 immunohistopathology, cell viability assay, qRT-PCR, RNA sequencing, gene set enrichment analysis
50 (GSEA) and live cell cycle tracking using *Fucci2BL* were performed.

51 **Results and limitations:** ADT resulted in CRPC spheroids with CK5⁺ CK8⁺ cells, up-regulated stem-
52 cell transcription factors, steroidogenic and neurogenic pathways and down-regulated AR-target
53 genes, interferon, cell cycle, cell division and circadian pacemaker pathways. Enzalutamide-treated
54 spheroids transitioned to G₀ and AR protein was decreased but not AR mRNA. Moreover, ADT
55 decreased both ACE2 and TMPRSS2, host cell viral entry factors for the severe acute respiratory
56 syndrome (SARS) SARS-CoV-2.

57 **Conclusions:** This study identified a new dormant CRPC basal-luminal hybrid prostate cancer cell
58 and gene signature which may be targeted to eradicate dormant CRPC bone metastases in order to
59 prevent disease recurrence. The PDX organoids can be used also to screen for therapies that reduce
60 ACE2 and TMPRSS2 expression thus suppressing viral load of SARS-CoV-2 and its variants.

61 **Patient Summary:** In organoids, or mini-tumors, established from prostate cancer bone metastases,
62 a novel type of dormant ADT-resistant cell with specific gene changes emerged which may be targeted
63 to eradicate dormant metastases before they can progress. ADT also reduced the cell factors required
64 for SARS-CoV-2 or its variants to infect its host cells and thus may reduce COVID-19 disease severity.

65

66

67 **Introduction (381 -> 308)**

68
69 Over 80% of advanced prostate cancer (PCa) patients develop bone metastases. Standard-
70 of-care androgen deprivation therapies (ADTs), such as enzalutamide, can be helpful initially to
71 prolong life, however, the majority of patients with bone metastases inevitably develop ADT resistance
72 known as castration-resistant prostate cancer (CRPC). As a result, many CRPC patients experience
73 significant morbidity including debilitating fractures and severe bone pain. Established prostate cancer
74 cell lines have been used as cost-effective and readily available *in vitro* models of prostate cancer,
75 however, they do not recapitulate the full complexity and heterogeneity of prostate tumors¹⁻⁵.
76 Therefore, we and other investigators have established patient-derived xenograft (PDX) models
77 through the transplantation of patient tumor samples into immunocompromised mice⁶⁻¹⁴.

78
79 Establishing models from prostate cancer patient tumors has been challenging because
80 cancer cells often become senescent upon isolation^{3, 6, 9, 15}. 3D organoid culture systems were
81 developed by the Clevers group for colorectal cancer organoids which transformed the field by
82 enabling reproducible cultures that provide niche-specific growth factors for patient-derived tumor
83 cells¹⁶⁻¹⁹. Prostate organoids retained the histopathological and functional traits of their origin including
84 gene expression profile, androgen responsiveness, and drug resistance^{20-24 25}.

85
86 Recently a connection between prostate cancer and coronavirus disease 2019 (COVID-19)
87 was revealed via transmembrane protease serine 2 (TMPRSS2). TMPRSS2 occurs as a gene fusion
88 with ETS family transcription factors in over 2/3 of prostate cancer patients²⁶. Severe acute respiratory
89 syndrome coronavirus 2 (SARS-CoV-2), the virus that causes COVID-19, infects cells using its S
90 protein which binds to its receptor, angiotensin-converting enzyme 2 (ACE2), on host cells²⁷.
91 TMPRSS2 was shown to be required for proteolytic processing the S protein once it is bound to ACE2
92 to allow fusion of the virus with the cell²⁷.

93
94 We report the characterization of a new ADT-resistant population and gene signature showing
95 androgen signaling-dependent SARS-CoV-2 host entry factors in *ex vivo* models of advanced prostate
96 cancer organoids.
97
98

99 **Methods (596 -> 438)**

100 **Patient-derived xenograft model and 3D organoid culture**

101 This study was carried out in strict accordance with the approval by the University of California
102 San Diego (UCSD) Institutional Review Board (IRB). Informed consent was obtained from all human
103 participants. A surgical prostate cancer bone metastasis de-identified specimen was harvested from
104 a patient who progressed to castrate resistant bone metastatic prostate cancer which we called
105 Prostate Cancer San Diego 1 (PCSD1). Intra-femoral injection of PCSD1 was performed to establish
106 a patient-derived xenograft (PDX) model^{11, 12, 28}. All animal protocols were performed under a UCSD
107 animal welfare IACUC approved protocol.

108 **Organoid growth**

109 PCSD1 tumor cells were embedded in a dome of growth factor reduced Matrigel (BD
110 Biosciences) at a seeding density of 50,000 cells per 40 μ L of Matrigel. 3D Organoid cultures grown
111 in prostate organoid medium¹⁷ with the addition of fetal bovine serum. DHT and Enzalutamide were
112 added to the medium at a final concentration of 1 nM and 10 μ M, respectively. The vehicle control was
113 0.1% (v/v) DMSO in culture medium. The epithelial cyst lumen diameter, cyst counts, spheroid area,
114 and spheroid counts were determined using a Keyence BZ-X710 microscope (Keyence Corporation).

115

116 **Quantitative RT-PCR**

117 Custom-designed human-specific primers were used for AR, prostate specific antigen (PSA)
118 and PSMA as previously described¹¹. Human and mouse-specific ACTB-specific primers were used
119 as an internal reference control for qPCR¹². Positive control RNA included human prostate RNA
120 (Clontech).

121

122 **RNA Sequencing Analysis and Bioinformatics**

123 RNA sequencing was performed on bulk RNA from the organoids and sequenced with 100
124 basepair (bp) paired end reads (PE100) to a depth of approximately 25 million reads per sample on
125 an Illumina NovaSeq 6000. The goal of the RNA sequencing was to identify genes responsive to ADT
126 through analysis strategies that could take into account the heterogeneity across organoid cultures.
127 Recognizing that each organoid potentially represented a different clone within the cancer, a query-
128 based analysis method was developed to accommodate for inter-organoid variability. Genes were first
129 filtered by consistent direction of response across organoid experiments 1 and 2, and then ranked by
130 degree of fold change and consistency of their response to the androgen deprivation treatments.

131

132 **Immunohistopathology**

133 The PCSD1 organoids were harvested and processed using a spin down method as previously
134 described²⁹.

135

136 **Live cell cycle imaging**

137 The cell cycle phase was determined by lentiviral bicistronic florescent, ubiquitination-based
138 cell cycle indicator reporter (*Fucci2 BL*) system. The *Fucci2 BL* expression vector was designed and
139 generated to have mVenus-hGem(1/110) and mCherry-hCdt1(30/120) in Pcdh-T2A-copGFP (SBI
140 Systems Biosciences) as previously reported³⁰.

141

142 **Statistical analysis**

143 Statistical significance for all the experiments was determined using the Student's t-test.

144

145 Further details for each method are provided in the Supplementary material.

146

147 **Results (1,188, needs to be 966)**

148

149 **PDX Organoids Recapitulate Heterogeneity and Androgen Deprivation Therapy Resistance of**
150 **the Patient's Tumor.**

151 Organoids were grown from the PDX, PCSD1, using intra-femoral xenograft tumor cells
152 (Figure 1A). Small gland-like structures were observed in PCSD1 organoids and xenografts (Figure
153 1.B). These were similar to tumor areas that were Gleason grade 10 (5+5) prostate cancer in the
154 donor patient's prostatectomy specimen. PCSD1 organoids consisted of a heterogeneous mix of multi-
155 cellular epithelial cysts and spheroids (Figure 1C).

156 Prostate epithelial cells typically require DHT to develop and function properly. Accordingly,
157 the average cyst lumen diameter was significantly greater ($P < 0.05$) with DHT (Figure 2) compared
158 to no DHT and was significantly decreased ($P < 0.05$) with 10 μM enzalutamide compared to vehicle
159 control. The total number of epithelial cysts was significantly increased ($P < 0.05$) plus DHT and
160 decreased by 10 μM enzalutamide ($P < 0.05$). PCSD1 organoid cultures also contained spheroids,
161 the cell-filled clusters which made up the majority of the organoids. By week 4, no DHT ($P < 0.0001$)
162 or enzalutamide decreased the average area of spheroids ($P < 0.0001$). There was no significant
163 difference in total number of spheroids under any of the treatment conditions. ADT-resistance of the
164 spheroids was confirmed in Alamar Blue viability assays (Figure S3).

165
166 **Androgen Deprivation Increased AR mRNA but Reduced AR protein and PSA in PDX PCa**
167 **Organoids.**

168 In organoids without DHT or with enzalutamide, AR mRNA levels increased as seen in qPCR
169 assays (Figure 3A). In contrast, AR protein levels were low in the enzalutamide-treated organoids
170 (Figure 3B). As expected, AR protein was in the nucleus with DHT (Figure 3B).

171 The effect of androgen deprivation on PSA, a transcriptional target of AR, and PSMA were
172 evaluated. Low PSA and high PSMA mRNA expression in the organoids were consistent with the
173 levels in the donor patient and PCSD1 PDX^{11, 12}. PSA protein expression was heterogeneous in

174 PCSD1 organoids as was seen previously in PCSD1 PDX¹². Androgen deprivation (no DHT or
175 +DHT/Enza) reduced PSA mRNA expression and protein (Figure 3C-E).

176
177 **Gene Expression Profiles from PDX Organoids under ADT Reveal Down-Regulation of**
178 **Cell Cycle, Circadian Pathways, and SARS-CoV-2 Host Cell Entry Factors, TMPRSS2 and ACE2.**

179 To define the global gene expression landscape of the organoids under androgen deprivation
180 we performed whole transcriptome RNA sequencing. The bioinformatics analysis strategy was to
181 compare gene expression in organoids with AR signaling, that is grown plus DHT, or in Vehicle plus
182 DHT, to those with no AR signaling, i.e., no DHT or plus Enzalutamide. This strategy yielded an ADT-
183 resistance signature of 787 differentially expressed genes: 312 genes Down-regulated with high
184 average expression, or high RPKM, 206 genes Down-regulated, low RPKM, 171 genes Up-regulated,
185 high RPKM and 98 genes Up-regulated, low RPKM. Hierarchical, unsupervised clustering of genes
186 was performed on the filtered gene lists of the four gene expression patterns (Figures 4, 5 and Figure
187 S4). Inspection of the heatmaps revealed significant down-regulation under ADT of prostate tissue
188 and known AR-target genes such as *TMPRSS2*, *KLK3(PSA)* (Table 1). Interestingly, *ACE2*, the host
189 receptor for the SARS-CoV-2 “S” protein and *DPP4*, the MERS-CoV host receptor were also down-
190 regulated by ADT.

191
192 ADT significantly down-regulated genes involved in cell cycle, cell division, mitosis and mitotic
193 spindle structure and function (*AURKA*, *AURKB*, *CCNA2*), DNA synthesis and repair (*PAPRP9*,
194 *BRCA1*), circadian clock gene *PER1* (Figure 4B), and an increase of two negative regulators of the
195 circadian clock (*BHLHE41*, *ARNTL2*) (Figure 5B). Notably, the glucocorticoid steroid hormone
196 receptor, *GR*, which can reset the circadian clock, was also down-regulated (Figure 4B).

197
198 ADT significantly altered genes in the following signaling pathways: Interferon signaling with
199 down-regulation of *IRF7* and *STAT1*, which are involved in anti-viral response (Figure 4A); WNT

200 signaling with down-regulation of *WTIP*, *LBH*, *WNT3*, and up-regulation of *WNT4* (Figure 4 and 5);
201 epithelial to mesenchymal transition (EMT) with down-regulation of *PARD6* (Figure 4B). Interestingly,
202 ADT led to up-regulation of genes involved in receptor tyrosine kinase (RTK) and serine/threonine
203 kinase signaling and growth such as *EGFR*, *PIM1*, G-protein coupled receptor (GPCR) signaling
204 (*RGS2*) and Cytokine signaling (*TNFRSF21*, *TNFS8*, *TGFB3*) (Figure 5). Many of these are actionable
205 targets.

206
207 ADT led to significant upregulation of genes involved in lipid metabolism, cholesterol, and
208 steroid hormone biosynthesis including *HSD3B1*, (Figure 5). Intriguingly, there was significant
209 upregulation of genes involved in neuronal development and synaptic function (*SEMA5A*, *SEMA3E*).
210 Consistent with this was downregulation of *SLITRK5*, an inhibitor of neuronal growth cone migration.
211 Notably, ADT up-regulated *NRP1*, a pro-nociceptive factor and another SARS-CoV-2 receptor. Finally,
212 ADT led to upregulation of developmental transcription factors involved in stem cells and cancer stem
213 (*ETV4*, *SOX9*, *FOXO1*, *FOXO3*).

214
215 Gene set enrichment analysis (GSEA) identified significantly down-regulated functional
216 pathways include interferon, cell cycle, cell division, mitosis, DNA damage response and cytokine
217 response. Significantly up-regulated functional pathways include neurogenesis, development and
218 differentiation, lipid metabolic process, partial apoptotic response and signal transduction response to
219 stimulus (Figure 6.A). Enrichment ranged from 1.4-fold to 5.4-fold with p-values ranging from 0.032
220 (circadian clock) up to 2.6E-09 (interferon signaling) and 5.8E-11 (cell cycle) (Figure 6B-E, Table 1).

221
222 **Androgen Deprivation Therapy Induced a Novel Population of Dormant CK5⁺CK8⁺**
223 **Basal-Luminal Hybrid Cells in PCSD1 Organoids.**

224 Analysis of prostate luminal and basal cell markers in PCSD1 organoids showed that ADT led to
225 mostly CK5⁺CK8⁺ cells with large CK5⁺ nuclei and CK8⁺ in the cytoplasm. PCSD1 organoids were
226 viable but Ki67 negative thus not proliferating (SI3 and Figure 7B). To determine the status of the cell
227 cycle in the live organoids over time we used the live cell cycle tracker system, *Fucci2BL* (Figure 7C).
228 The majority of PCSD1 organoids in +DHT/Enza shifted to G₁/G₀ phase while the rest of organoids
229 were green, and thus, in S/G₂/M phase (Figure 7C-D). Taken together, our results are consistent with
230 the live PCSD1 cells shifting to the G₀ phase over time, and thus, becoming dormant ADT-resistant
231 bone metastatic prostate cancer cells.

232

233 **Discussion (1333 except the yellow highlighted statement, needs to be 881)**

234

235 In this study, we established a new bone metastatic prostate cancer organoid model using tumor cells
236 from the patient-derived xenograft, PCSD1, and investigated their ADT response and mechanisms of
237 resistance to ADT. We captured the ADT-induced transition to castration resistant prostate cancer and
238 identified gene and protein expression changes culminating in dormant CRPC organoids. The
239 dormancy CRPC signature identified here may be targeted for novel combination drug treatments that
240 eradicate these dormant prostate cancer metastases and prevent further progression to recurrent
241 tumor growth and metastatic spread.

242 In our study, several features confirmed that the different 3D multi-cellular PCSD1 organoids
243 all arose from the purified PDX tumor cells. First, the PCSD1 PDX tumor cells had been engineered
244 in previous studies to stably express green fluorescent protein (GFP) and luciferase for *in vivo*
245 imaging¹². Accordingly, all of the PCSD1 organoids expressed GFP and luciferase. Second, PSA was
246 expressed in PCSD1 organoids but at low levels which was consistent with the donor patient and
247 PCSD1 *in vivo* PDXs.^{11, 12} Third, the PCSD1 organoids expressed AR mRNA which increased in the
248 CRPC organoids under androgen deprivation conditions previously seen in the PCSD1 PDX treated

249 with anti-androgen in vivo. Fourth, the organoids expressed the prostate marker proteins, PSA, the
250 prostate basal cell marker, CK5, and the prostate luminal cell marker, CK8. Fifth, whole genome RNA
251 sequencing showed the expression of prostate-specific genes such as KLK3 (PSA) and NKX3.1 and
252 decreased expression of well-known AR-target genes in the absence of AR-signaling, that is, in the
253 organoids No DHT or plus enzalutamide. (references Raheem 2011, Godebu 2014, Toth 2019)

254
255 We and others have established 3D organoid models in culture from patient tissues which retain the
256 stem cell and their progenitors and differentiated cells^{16-19, 22, 24, 25, 29, 31-35}. The hollow prostate epithelial
257 cysts and cell-filled, acinar spheroids which were observed in the PCSD1 organoids have also been
258 seen in organoids from other epithelial tissues such as breast, lung and colon^{18, 19, 36}. In breast cancer
259 3D culture models cancer cells which had less malignant properties tended to form epithelial cysts or
260 acini with a hollow lumen while more malignant cells tended to form cellular aggregates or filled acini
261 reminiscent of their growth as tumors in patients^{36, 37}. We postulated that the epithelial cysts may come
262 from a less malignant sub-population of tumor cells, whereas, the spheroids may arise from more
263 malignant cancer stem-like cells in the heterogeneous PDX tumor.

264
265 Strikingly, we found that while enzalutamide-treatment of organoids led to an increase in AR
266 mRNA there was a concomitant decrease in AR protein. This may have been due to direct binding
267 and inhibition of AR by enzalutamide which triggered AR protein degradation. A similar response was
268 described in Giridhar et al in which AR protein was continuously translated in prostate stem cells
269 treated with the anti-androgen, flutamide, but it was continuously degraded by the E3 ligase, MDM2,
270 and proteasome. Thus, the cells had no or low steady-state AR protein which was required to
271 maintain an AR negative, prostate cancer stem cell phenotype³⁸. Interestingly, our preliminary data
272 show that PCSD1 PDX and patient tumor cells have increased copy number of the MDM2 gene and
273 thus may have up-regulated this proteolytic pathway.

274

275 The novel ADT-resistant, dormant CRPC CK5⁺CK8⁺ hybrid cells induced in no DHT or
276 enzalutamide-treated organoids may be developmental intermediates or transition states that were
277 stably captured under ADT in the organoid culture conditions. In previous studies, prostate cells with
278 both basal and luminal markers CK5⁺CK18⁺ Intermediate cells have been observed in prostate
279 inflammatory atrophy (PIA)³⁹. Recently, PIA-like, low CD38-expressing, inflammation-associated
280 luminal cells are known to initiate prostate cancer⁴⁰. Such intermediates, or transition states, are found
281 in other cancers as well. Kroger *et al.* showed a hybrid epithelial to mesenchymal (E/M) transition state
282 which down-regulated both CK5 and CK8 which was highly tumorigenic in breast cancer cell lines
283 suggesting a model in which these transition states represent a spectrum in tumor lineage plasticity,
284 regeneration in response to damage and tumorigenicity^{41, 42}. Transcriptomic and protein analyses in
285 IHC and IFC revealed that the ADT resistant CK5⁺CK8⁺ hybrid epithelial cells had up-regulated stem-
286 cell transcription factors, steroidogenic and neurogenic pathways while down-regulating cell cycle, cell
287 division and circadian pacemaker machinery, as well as the SARS-CoV-2 host cell entry factors,
288 TMPRSS2 and ACE2. The *Fucci2BL* system live cell cycle tracker system allowed us for the first time
289 to follow the time course of ADT-induced changes in the cell cycle in live cells while maintaining critical
290 cell-cell interactions in the three-dimensional organoid structure. We postulate that this may more
291 accurately reveal the dynamic effects of ADT on the cell cycle *in vivo*. We showed that in the presence
292 of androgen such as DHT, the majority of the cells in the organoids were in S/G2/M and not actively
293 proliferating. With Enzalutamide, the organoids transitioned from S/G2/M to G0. This lack of
294 proliferation was confirmed by lack of Ki67 protein as shown by immunostaining of the organoids.
295 Therefore, enzalutamide treatment led to the emergence of a dormant, ADT-resistant hybrid basal-
296 luminal prostate cancer cell type in the organoids. The findings here tie together previous studies on
297 a rare population of prostate epithelial cells which were suggested to be an antecedent in the events
298 leading to prostate cancer with a new mechanism of castration resistance in patient-derived prostate
299 cancer organoids. The newly identified, castration-resistant, basal-luminal hybrid prostate cancer cells

300 may represent a type of treatment-emergent, transitional state between ADT-resistant dormancy and
301 re-current growth.

302
303 The dormancy CRPC gene signature identified in these PDX organoids revealed specific
304 genes and pathways that may be targeted alone or in combination to eradicate dormant CRPC before
305 further progression and recurrence to a more malignant, harder to treat disease.

306
307 Interestingly, we found that ADT down-regulated both of the SARS2-CoV-2 host factors,
308 TMPRSS2 and ACE2, which are required to mediate viral entry. This is the first study directly
309 demonstrating that a therapeutic anti-androgen down-regulated ACE2 in human cells. Androgen
310 regulation of ACE2 has been implicated in studies showing that male alveolar lung cells have higher
311 expression of AR, TMPRSS2 and ACE2 compared to female. It has been observed in studies from
312 multiple COVID-19 pandemic epicenters including Wuhan, China, Veneto, Italy and New York, USA,
313 that men have a worse COVID-19 disease course and higher mortality compared to women⁴³⁻⁴⁹. We
314 and others have postulated that the increased COVID-19 disease severity and death rate in men may
315 be due in part to increased TMPRSS2 and ACE2 expression in men. Furthermore, prostate cancer
316 cells which often have high levels of TMPRSS2 and co-express ACE2 on prostate tumor cells may
317 represent an additional male cancer vulnerability to SARS-CoV-2. Prostate cancer cells with high
318 TMPRSS2 and ACE2 may have a high level of SARS-CoV2 infection thus, acting as a SARS-CoV-2
319 infection accelerator and/or reservoir. In addition, cancer cells including prostate cancer cells down-
320 regulate HLA and evade immune surveillance. Therefore, SARS-CoV-2 infection of cancer cells may
321 allow the virus to evade the immune system especially prostate cancer cells which have high levels
322 of SARS2-CoV-2 host factors, TMPRSS2 and ACE2 which mediate viral entry. Therefore, prostate
323 cancer patients may not be able to clear the virus and may constantly shed virus as was reported
324 recently in another immunocompromised patient with CLL⁵⁰. Interestingly, analysis of prostate cancer
325 patients in Veneto, Italy who became infected with COVID-19 showed that patients on androgen

326 deprivation therapy (ADT) had overall less severe disease than prostate cancer patients not on ADT⁵¹.
327 They had fewer hospitalizations and a shorter disease course. These observations have led to three
328 currently ongoing clinical trials in which a short course of ADT is being given to patients who test
329 positive for SARS-CoV-2. Anti-androgen therapy may be used as a treatment to reduce TMPRSS2
330 and ACE2 expression and inhibit SARS-CoV-2 virus levels in both male and female patients.
331 Furthermore, ADT to reduce TMPRSS2 and ACE2 would be effective for reducing viral load of variants
332 of SARS-CoV2 and, therefore, could be a crucial weapon against the new variants that are arising
333 that can evade immune-based therapies.

334

335

336 **Conclusions (77 words)**

337

338 Androgen deprivation or enzalutamide treatment of PCa PDX organoids led to the emergence
339 of newly identified dormant castration resistant hybrid basal-luminal prostate cancer cells and dormant
340 CRPC gene signature showing decreased expression of both SARS-CoV-2 host cell viral entry factors,
341 TMPRSS2 and ACE2. PDX prostate cancer organoids can be used as models that more accurately
342 represent the tissue in vivo to screen for therapies that target dormancy in this new mechanism of
343 ADT resistance and also for therapies that reduce TMPRSS2 and ACE2, thus suppressing viral load
344 of SARS-CoV-2 and its variants.

345

346 **Take Home Message (40 words)**

347

348

349 **Acknowledgements**

350

351 This study was supported by the Leo and Anne Albert Charitable Foundation and JM
352 Foundation. We thank Drs. Jing Yang and Dr. Kay T. Yeung, UCSD Moores Cancer Center, for the

353 generous access to their microtome. We would also like to thank the following people from the Moores
354 Cancer Center shared resources teams for their assistance with our experiments: Kersi
355 Pestonjamas, Microscopy; Alfredo Molinolo, Sharmeela Kaushal, and Jim Salinas, Biorepository;
356 Valeria Estrada and Laarni Gapuz, Tissue Technology. Tissue Technology Shared Resource is
357 supported by a National Cancer Institute Cancer Support Grant (CCSG Grant P31CA23100). The
358 Keyence Model microscope was supported by the UCSD Cancer Center Microscopy Shared Facility
359 Specialized Support Grant P30 CA23100-28. This publication includes data generated at the UC San
360 Diego IGM Genomics Center utilizing an Illumina NovaSeq 6000 that was purchased with funding from
361 a National Institutes of Health SIG grant (#S10 OD026929). We especially thank Dr. Kristen Jepsen,
362 Director, of the IGM Genomics Center for their work to run our RNASeq samples. We are grateful for
363 the technical support of Jamieson lab members Jamillah Murtadha, Johnathan Hsu and Rejina
364 Roufegarinejad.

365

366 **Author Contributions**

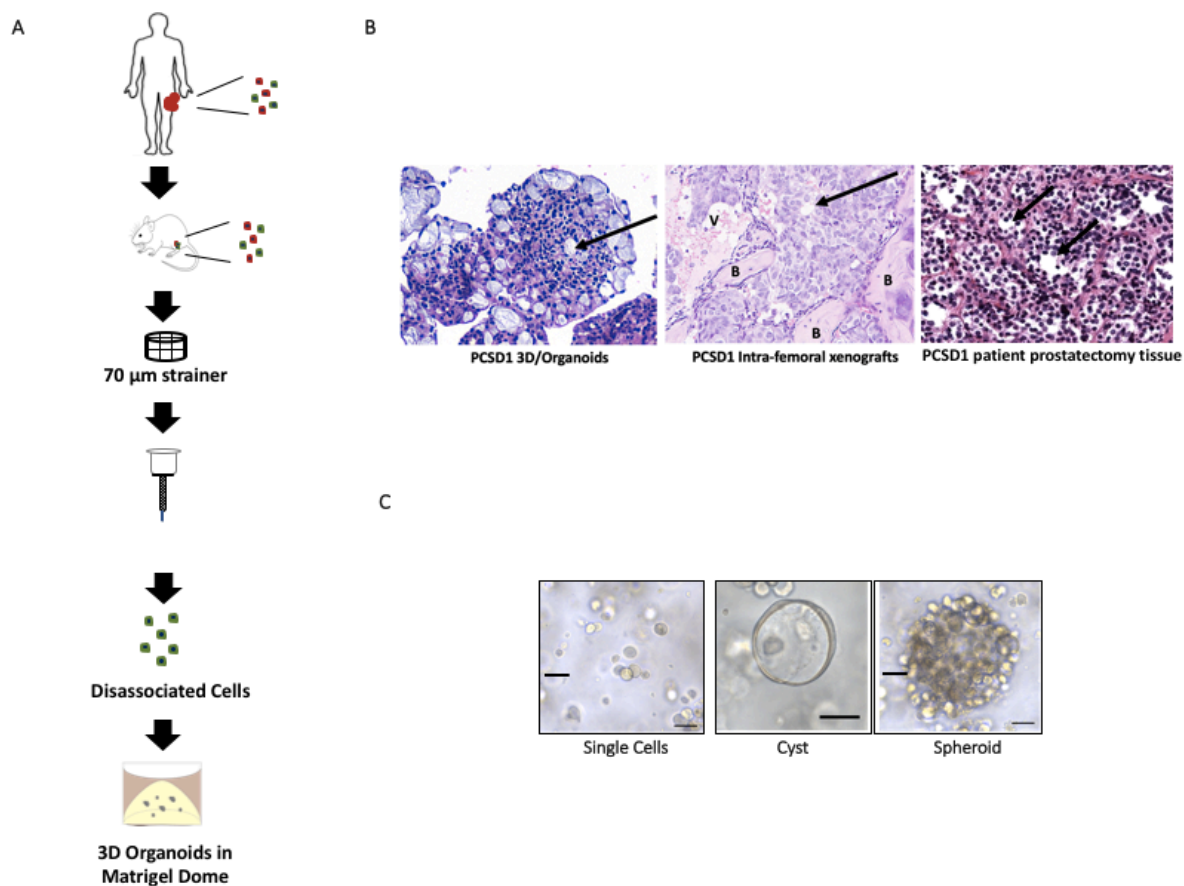
367 S.L, T.R.M, D.N.B and C.A.M.J conceived and designed the experiments and wrote the
368 manuscript. S.L, T.R.M, D.N.B and W.Y.Z established the 3-dimensional (3D) culture of patient-
369 derived organoids. C.A.M.J. and C.N.W established the patient-derived xenograft (PDX) model of
370 bone metastatic prostate cancer. C.N.W. and M.T.M performed intra-femoral injections of PCSD1 for
371 PDX tumor cells to make organoids. C.N.W, M.T.M., T.R.M., C.A. and A.Z maintained the PDX model
372 and performed tumor harvest. S.L, T.R.M, and D.N.B performed the ex vivo study to determine
373 dihydrotestosterone (DHT) and enzalutamide response. T.R.M, D.N.B and C.A developed and
374 performed quantitative cyst and spheroid analysis. S.L, D.N.B and M.T.M performed histological
375 analysis. S.L, M.T.M, C.A, O.M.G. and A.Z performed immunohistochemistry and immunofluorescent-
376 chemistry. G.P and K.M.L developed *Fucci2 BL* and provided lentiviral particles, expertise and advice.
377 T.R.M and D.N.B performed an enzalutamide dose response test. D.N.B and T.R.M. performed qRT-
378 PCR. N.A.C and T.R.M performed statistical analysis. C.H.M.J, C.J.K, A.A.K and C.A.M.J participated

379 in discussions and prepared IRB approval and human subject recruitment. A.A.K. performed
380 orthopedic surgery and provided the surgical specimens of bone metastatic prostate cancer. S.L,
381 T.R.M, D.N.B, M.T.M, N.A.C and C.A.M.J participated in the discussion of the results and manuscript
382 editing.

383

384 **Declaration of Interests**

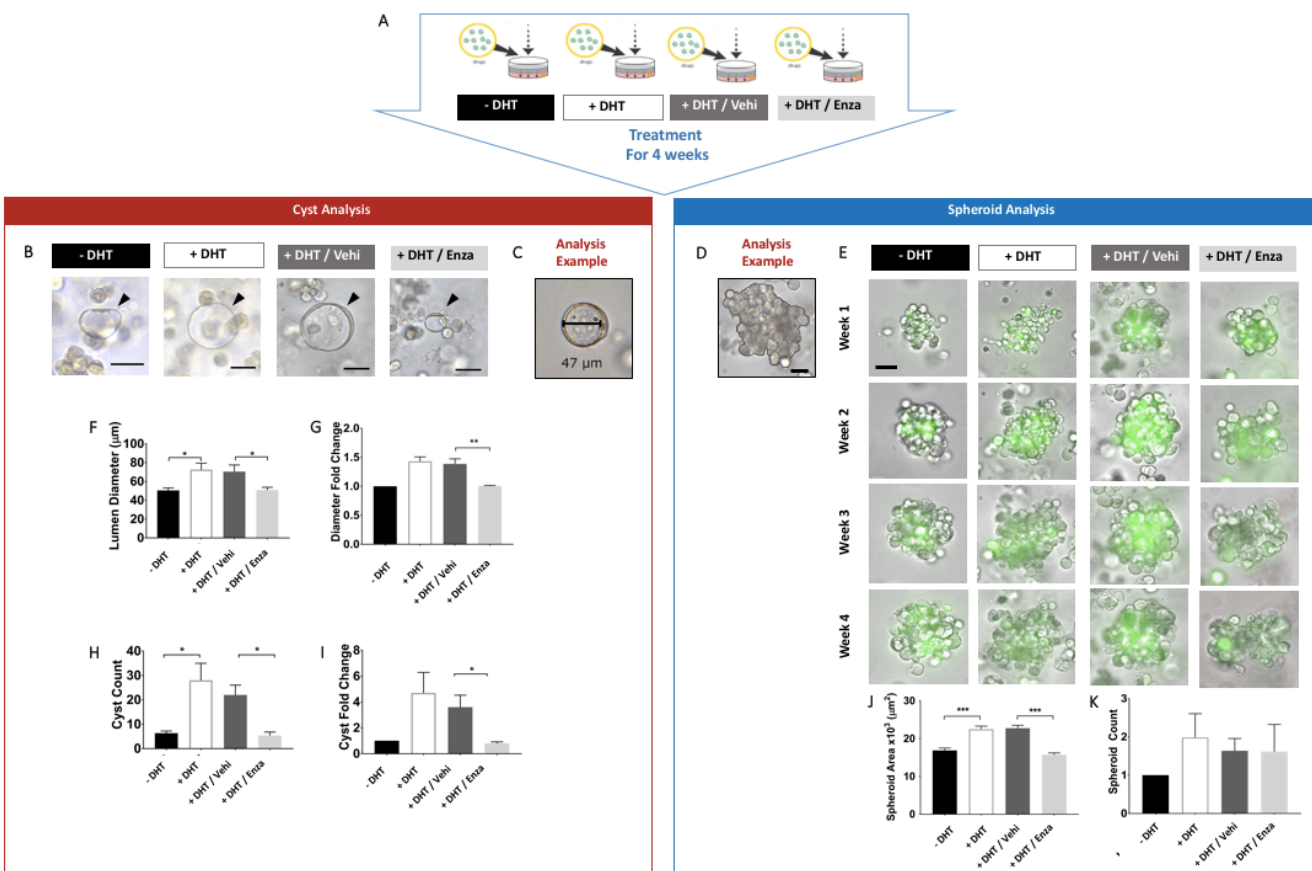
385 CJ reports investigator-initiated project funding from Calibr, Inc., Astellas, Medivation, and
386 Pfizer outside the submitted work. CK reports having stock ownership in Stratify genomics outside the
387 submitted work. All other authors declare no competing interests related to this study.

388 **Figure Titles and Legends**

389
 390 **Figure 1. PDX Organoids Recapitulate Cellular Heterogeneity and Histopathology of the**
 391 **Originating Patient's Prostate Cancer.**

392 (A) Workflow to establish and optimize 3D organoids from patient-derived xenograft (PDX) model of
 393 prostate cancer bone metastasis. (B) Representative images of hematoxylin and eosin (H&E) stained
 394 samples of PCSD1 organoids vs PCSD1 intra-femoral xenografts. Black arrows point to small gland-
 395 like structures seen in both the organoids and xenografts growing in the femur. B indicates bone, V
 396 indicates blood vessel. H&E images are shown at 10X magnification. (C) A heterogeneous mix of
 397 PCSD1 tumor cells grown in 3D organoid cultures consisting of single cells, hollow epithelial cysts,
 398 and cell-filled spheroids. Brightfield microscope images of single cells and the spheroid are at 10X
 399 magnification and the cyst is at 20X magnification. Scale bars represent 50 μm .

400



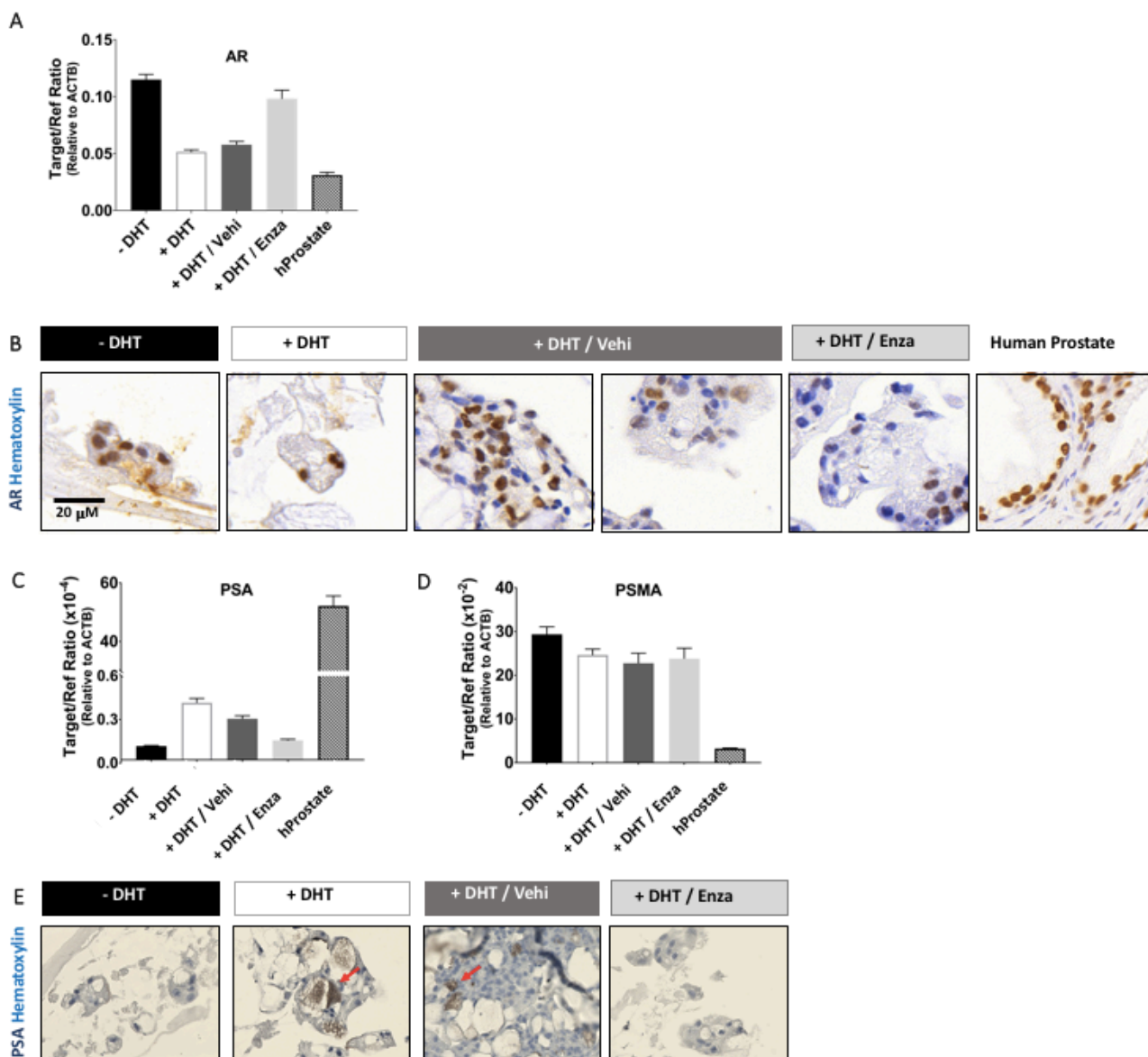
401
402 **Figure 2. PDX Organoids Recapitulate the Androgen Deprivation Therapy Resistance of the**
403 **Patient.**

404 (A) Experimental design of 3D cultures of PCSD1-GFP/Luciferase+ organoids under four treatment
405 conditions: -DHT, +DHT (1 nM), +DHT/Vehicle (1 nM/0.1% DMSO), and +DHT/Enzalutamide (1 nM/10
406 μM). PCSD1 organoids in each treatment group were imaged weekly with a Keyence digital
407 microscope for four weeks. (B) A representative image of cyst in each treatment condition after 4
408 weeks of treatment. (C) A measurement example of cyst lumen diameter using the Hybrid Cell Counter
409 software. Scale bar for spheroid image is 50 μm . After measurement of cyst lumen diameter, the
410 number of epithelial cysts greater than 50 μm in size was quantified in each culture. (D) An analysis
411 example of spheroid area using the Hybrid Cell Counter software. Scale bar for spheroid image is 100
412 μm . (E) A representative image of spheroid in each treatment condition at week 1, 2, 3, and 4 of
413 treatment. (F) Average lumen diameter of cysts, (E) Fold changes in lumen diameter, (H) number of

414 cyst count, (I) Fold changes in cyst count. (J) Average spheroid area, (K) The number of spheroids
415 under four treatment conditions: -DHT, +DHT (1 nM), +DHT/Vehicle (1 nM/0.1% DMSO), and
416 +DHT/Enzalutamide (1 nM/10 μ M). For fold change analysis in (G), (I) and (K), quantified values were
417 normalized to the DHT- condition. Data represent the mean from four independent (n=4) experiments
418 performed in triplicate \pm SEM. A student's t-test was used to determined statistical significance
419 (*indicate $P < 0.05$, ** indicates $P < 0.01$ *** indicated $P < 0.0001$).

420

421



422

423 **Figure 3. Androgen Deprivation Reduces Levels of AR protein and PSA gene expression in**
 424 **PDX Organoids.**

425 (A) Quantitative RT-PCR analysis for AR level in PCSD1 3D organoids under the four treatment
 426 conditions: -DHT, +DHT (1 nM), +DHT/Vehicle (1 nM/0.1% DMSO), and +DHT/Enzalutamide (1 nM/10
 427 μ M). Human Beta Actin was used as the internal control, reference gene ($\Delta\Delta C_t$ Target /
 428 Reference). (B) IHC analysis of AR expression in PCSD1 3D organoids. Representative digital
 429 microscope images are shown of AR IHC staining performed on 4% paraformaldehyde fixed, paraffin

430 embedded 5 μm sections from four culture conditions. Human prostate tissue was used as a positive
431 control. (C) Quantitative RT-PCR analysis for PSA level in PCSD1 3D organoids. (D) Quantitative RT-
432 PCR analysis for PSMA level in PCSD1 3D organoids under the four treatment conditions. Graphs
433 represent one experiment performed in duplicate. (E) Immuno-histochemical (IHC) analysis of PSA
434 expression in PCSD1 3D organoids. Red arrows point to PSA positive staining. Representative digital
435 microscope images are shown of PSA IHC staining performed on 4% paraformaldehyde fixed, paraffin
436 embedded 5 μm sections from four culture conditions.

437

438

439

440

441

442

443

444

445

446

447

448

449

450

451

452

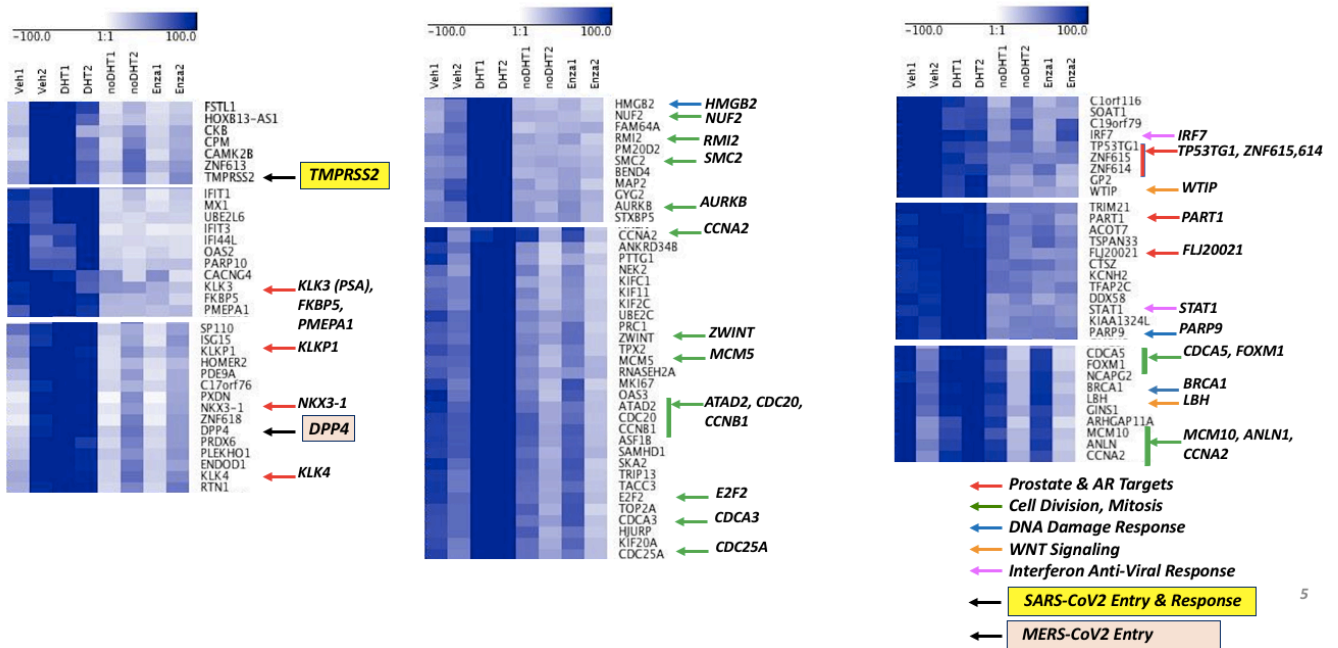
453

454

455

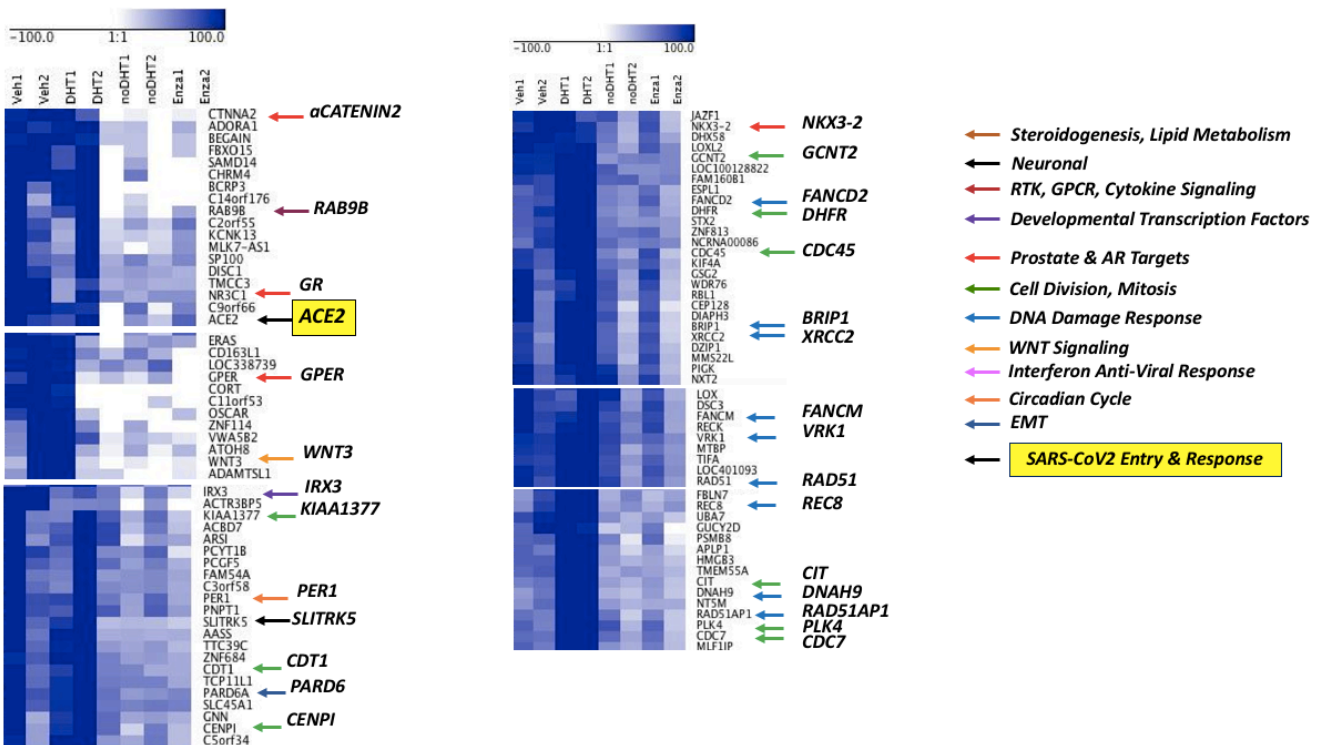
456

A. Down-Regulated Genes, High RPKM



457

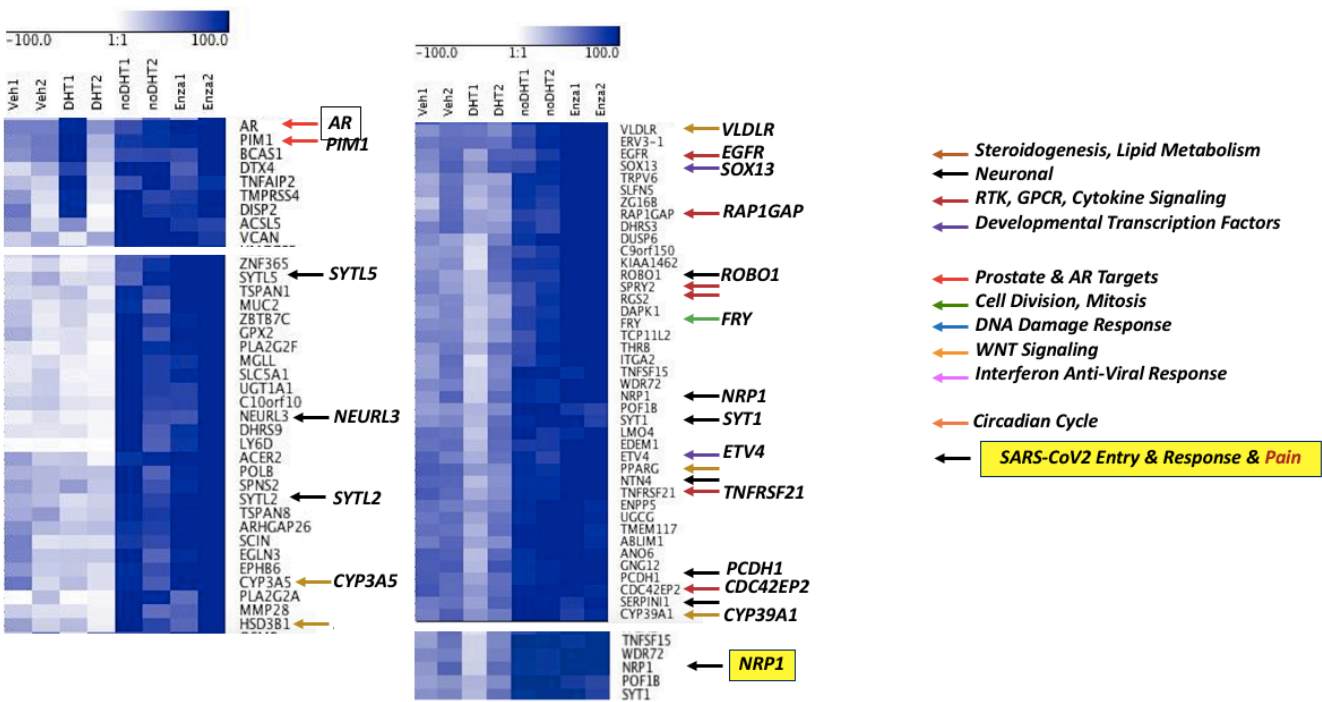
B. Down-Regulated Genes, Low RPKM



458

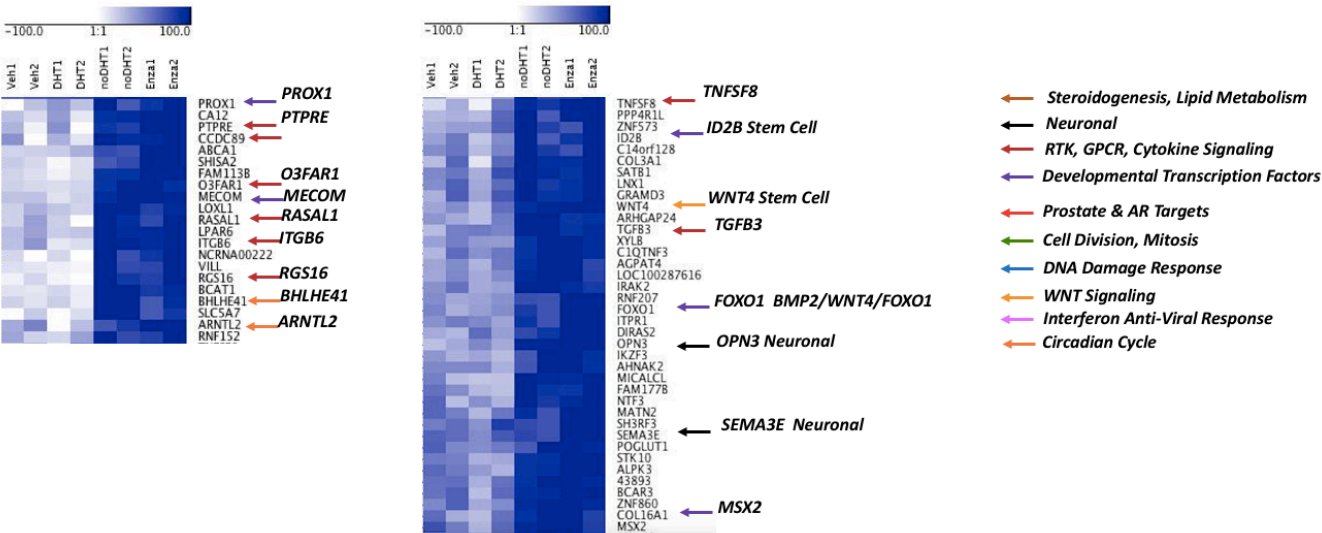
459 **Figure 4. Gene Expression Profiles from PDX Organoids under ADT Reveal Down-Regulation**
460 **of Cell Cycle and Circadian Pathways, and SARS-CoV-2 Host Cell Entry Factors, TMPRSS2 and**
461 **ACE2.** Heatmaps organized by hierarchical clustering for significantly down-regulated genes in
462 PCSD1 organoids under two androgen treatment conditions: (1) Veh (+DHT/Vehicle – 1 nM/0.1%
463 DMSO), (2) DHT (+DHT – 1 nM) and PCSD1 organoids under two androgen deprivation treatment
464 conditions: (3) noDHT (-DHT) and (4) Enza (+DHT/Enzalutamide – 1 nM/1 μ M). (A) Significantly down-
465 regulated genes with high normalized read counts (RPKM). Genes from functional categories enriched
466 in the differential genes marked with arrows: prostate & AR targets (red); cell division, mitosis (green);
467 DNA damage response (blue); WNT signaling (orange); interferon anti-viral response (pink); SARS-
468 CoV-2 entry & response (black arrow with yellow box) and MERS-CoV entry (black arrow with beige
469 box). (B) Significantly down-regulated genes with low overall RPKM. Genes from functional categories
470 enriched in the differential genes marked with arrows: steroidogenesis, lipid metabolism (brick red);
471 neuronal (black); RTK, GPCR, cytokine signaling (red); developmental transcription factors (purple);
472 prostate & AR targets (bright red); cell division, mitosis (green); DNA damage response (blue); WNT
473 signaling (light orange); interferon anti-viral response (pink); circadian cycle (orange); EMT (dark blue)
474 and SARS-CoV-2 entry & response (black arrow with yellow box).
475

A. Up-Regulated Genes, High RPKM



476

B. Up-Regulated Genes, Low RPMK



477

478

479 **Figure 5. Gene Expression Profiles from PDX Organoids under ADT Reveal Up-Regulation of**
480 **Neurogenic, Steroidogenic Genes and Stem Cell Transcription Factors.**

481 Heatmaps organized by hierarchical clustering for significantly up-regulated genes in PCSD1
482 organoids under two androgen treatment conditions: (1) Veh (+DHT/Vehicle – 1 nM/0.1% DMSO), (2)
483 DHT (+DHT – 1 nM) and PCSD1 organoids under two androgen deprivation treatment conditions: (3)
484 noDHT (-DHT) and (4) Enza (+DHT/Enzalutamide – 1 nM/1uM). (A) Significantly up-regulated genes
485 with high normalized read counts (RPKM). Genes from functional categories enriched in the differential
486 genes marked with arrows: steroidogenesis, lipid metabolism (brick red); neuronal (black); RTK,
487 GPCR, cytokine signaling (brown); developmental transcription factors (purple); prostate & AR targets
488 (red); cell division, mitosis (green); DNA damage response (blue); WNT signaling (orange); interferon
489 anti-viral response (pink); circadian circle (dark orange) and SARS-CoV-2 entry & response & pain
490 (black arrow with yellow box). (B) Significantly up-regulated genes with low overall RPKM. Genes from
491 functional categories enriched in the differential genes marked with arrows: steroidogenesis, lipid
492 metabolism (brick red); neuronal (black); RTK, GPCR, cytokine signaling (dark brown); developmental
493 transcription factors (purple); prostate & AR targets (bright red); cell division, mitosis (green); DNA
494 damage response (blue); WNT signaling (light orange); interferon anti-viral response (pink) and
495 circadian cycle (orange).

496

497

498

499

500

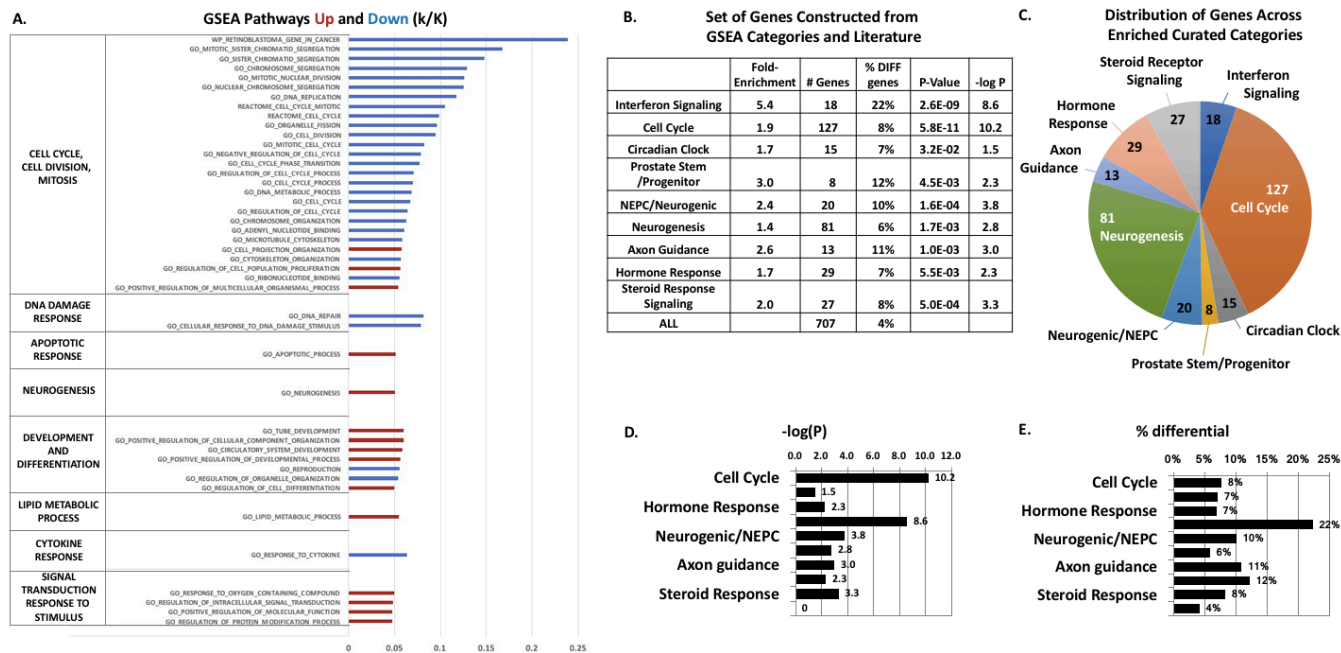
501

502

503

504

505



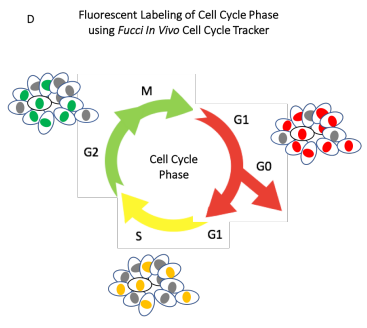
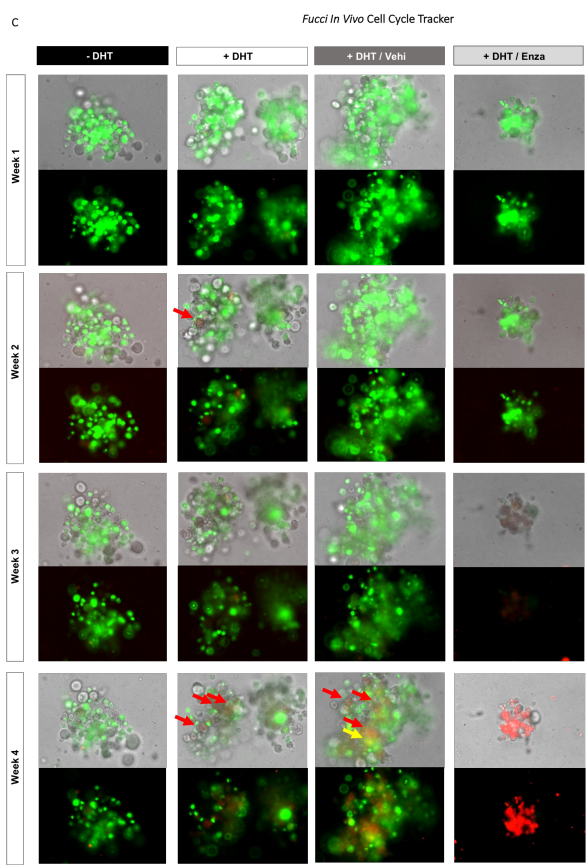
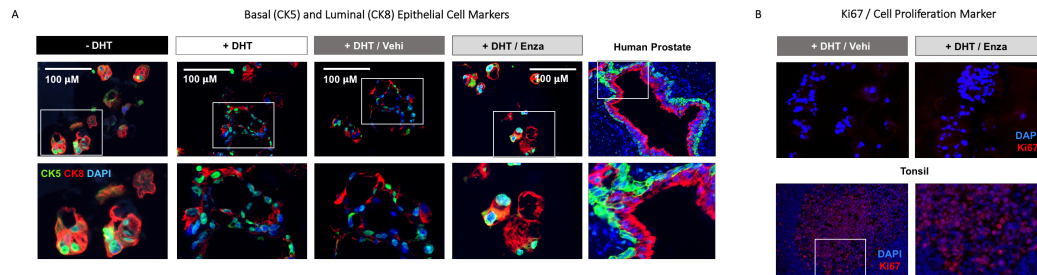
506

507 **Figure 6. Gene Set Enrichment Analysis (GSEA) Shows Differentially Expressed Genes in**
 508 **Interferon Signaling, Cell Cycle, Circadian Clock, Prostate Stem/Progenitor, NEPC/Neurogenic,**
 509 **Neurogenesis, Axon Guidance, Hormone Response and Steroid Receptor Signaling. (A) List of**
 510 **up-regulated (red) and down-regulated (blue) pathways evaluated using GSEA. (B) Enrichment scores**
 511 **for unified gene sets constructed from overlapping GSEA functional categories and literature. (C) Pie**
 512 **chart showing distribution of genes across enriched categories. (D) Bar graph showing $-\log(P)$ for**
 513 **each category, P calculated using Fisher's exact test. (E) Bar graph showing fold-enrichment for each**
 514 **category.**

515

516

517



518

519

520 **Figure 7. Androgen Deprivation Therapy-Resistant Population of PCSD1 Organoids are**
521 **CK5⁺CK8⁺ Basal-Luminal Hybrid and Dormant Cells.**

522 (A) Confocal FV1000 images of IFC that was performed on PCSD1 3D organoids and normal human
523 prostate cancer control tissue to visualize the prostate epithelial cell markers: Cytokeratin 8 (CK8), a
524 luminal epithelial cell protein, and Cytokeratin 5 (CK5), a basal epithelial cell protein along with DAPI
525 nuclear stain. Top five panels: PCSD1 3D organoids and patient prostate cancer tissue showed
526 cytoplasmic CK8 protein (red), and perinuclear and nuclear CK5 protein (green). DAPI stained the
527 nuclei (blue). Inset (white square) shows further magnified image of organoids with cytoplasmic CK8
528 and perinuclear CK5 in the same cells. In the PCSD1 organoids, immunofluorescent cytochemical
529 (IFC) analysis of CK5 and CK8 revealed heterogeneous expression patterns. Confocal microscope
530 imaging of the control tissue, normal human prostate, showed the expected pattern of CK5⁺ basal
531 cells and CK8⁺ luminal cells in glandular structure. (B) Confocal FV1000 images of IFC that was
532 performed on PCSD1 3D organoids and normal tonsil positive control tissue to visualize the cell
533 proliferation marker, Ki67, in two treatment conditions of +DHT/Vehi and +DHT/Enza at week4. Red
534 color indicates Ki67 protein present. (C) Time course of cell cycle stages in live PCSD1 organoids
535 under the four treatment conditions. Representative images in each treatment condition at week 1, 2,
536 3, and 4 of treatment of PCSD1 organoids stably expressing the *Fucci2 BL* bicistronic fluorescent,
537 ubiquitination-based cell cycle indicator reporter system showing three cell cycle phases: G₁ / G₀ by
538 red fluorescence, G₁/S by yellow fluorescence, and S/G₂/M by green fluorescence. The images of
539 bright-field, red fluorescent channel and green fluorescent channel were taken and merged. (D) The
540 *Fucci2 BL* fluorescent, ubiquitination-based cell cycle indicator reporter system visualizes the phase
541 of cell cycle shown by colorimetric signal of red, yellow and green fluorescence for G₁, G₁/S and
542 S/G₂/M, respectively.

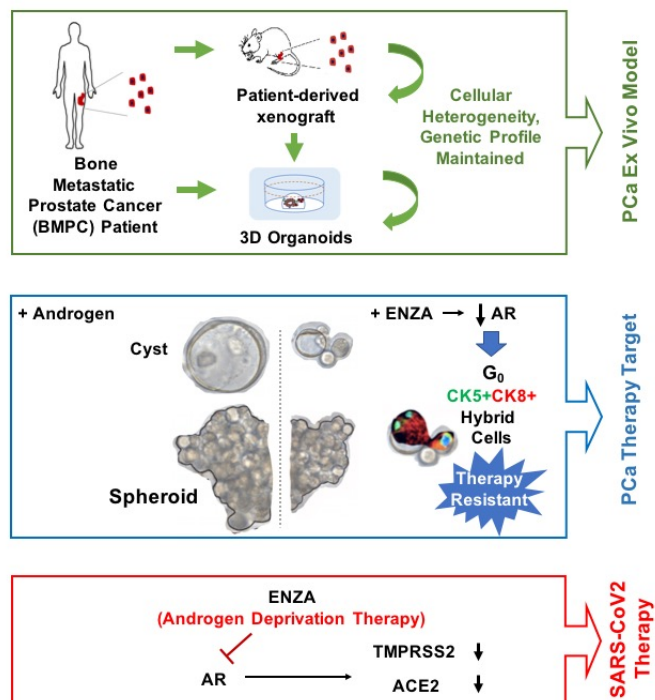
543

544

HIGHLIGHTS

- Patient-derived xenograft (PDX) models for bone metastatic prostate cancer and three-dimensional (3D) organoids (mini-tumors) more predictive pre-clinical research platforms.
- PDX Organoids used to test androgen deprivation therapy (ADT) resistance mechanisms.
- Novel hybrid basal-luminal cells that were ADT resistant, quiescent prostate stem-cell like gene expression profile.
- ADT decreased expression of the severe acute respiratory syndrome (SARS) SARS-CoV-2 host cell viral entry factors, TMPRSS2 and ACE2 as well as the Middle East respiratory syndrome (MERS) MERS-CoV receptor, DPP4 as well as anti-viral interferon response.
- Therefore, PDX organoids may be used to screen for novel therapies that target mechanisms of ADT resistance in PCa and for therapies that reduce TMPRSS2 and ACE2 expression and thus block SARS-CoV2 infection.

GRAPHICAL ABSTRACT



547 **Table 1. Selected genes of interest in ADT-signature from PDX PCSD1 organoids**
 548

Direction of Gene Expression Change with ADT	Number of Genes (787 Total)	Category	Selected Genes of Interest
Down	518		
		Prostate and AR-target genes	<i>TMPRSS2, KLK3(PSA), KLK4, KLKP1, FKBP5, PMEPA1, NKX3-1, TP53TG1, ZNF614, ZNF615, PART1, FLJ20021, GR, GPER, NKX3-2</i>
		Cell cycle, cell division, mitosis and mitotic spindle structure and function	<i>NUF2, RMI2, SMC2, AURKA, AURKB, CCNA2, ZWINT, MCM5, ATAD2, CDC20, CCNB1, E2F2, CDC3A, CDC25A, KIA1377, CDT1, CENPI, GCNT2, DHFR, CDC45, CIT, PLK4, CDC7</i>
		DNA synthesis and repair	<i>HMGB2, PAPRP9, BRCA1, FANCD2, BRIP1, XRCC2, FANCM, VRK1, RAD51, REC8, DNAH9, RAD51AP1</i>
		Circadian clock	<i>PER1</i>
		Interferon signaling	<i>IRF7, STAT1</i>
		WNT signaling	<i>WTIP, LBH, WNT3</i>
		Epithelial to mesenchymal transition (EMT)	<i>PARD6</i>
		SARS-CoV2 Host Viral Entry factors	<i>TMPRSS2, ACE2</i>
Up	269	Serine/threonine kinase signaling and growth	<i>EGFR, PIM1, RAPGAP1, SPRY2, CDC42EP2, PTPRE, CCDC89, O3FAR1, RASAL1, ITGB6, RGS16</i>
		G-protein coupled receptor (GPCR) signaling	<i>RGS2</i>
		Cytokine signaling	<i>TNFRSF21, TNFS8, TGFB3</i>
		Lipid metabolism, cholesterol, and steroid hormone biosynthesis	<i>CYP3A5, HSD3B1, VLDLR, PPARG, CYP39A1</i>
		Neuronal function and development	<i>NRP1, ROBO1, SYT1, NTN4, PCDH1, SERPINI1, SYTL5, SYTL2, SEMA5A, OPN3, SEMA3E</i>
		Developmental transcription factors in stem cells and cancer stem cells	<i>ETV4, SOX13, MSX2, SOX9, FOXO1, FOXO3, PROX1, MECOM, ID2B, GATA2</i>

549

550

Category	Fold Enrichment	P-value	Differential (# Genes)			NO CHANGE (% Genes)			Total # Genes with Reads		
			UP	DOWN	Total	%	HIGH	LOW		Total	
Interferon Signaling	4.9	2.0E-08	0	18	18	22.8	40	21	61	77.2	79
Cell Cycle	1.7	1.5E-07	18	109	127	7.8	985	519	1,504	92.2	1,631
Circadian Clock	1.6	9.3E-02	7	8	15	7.2	113	79	192	92.8	207
Prostate Stem /Progenitor	2.6	1.1E-02	5	3	8	12.1	22	36	58	87.9	66
NEPC/ Neurogenic	2.2	1.9E-03	6	14	20	10.0	85	95	180	90.0	200
Neurogenesis	1.3	3.3E-02	41	40	81	5.9	627	655	1,282	94.1	1,363
Axon Guidance	2.4	3.2E-03	12	1	13	11.1	50	54	104	89.9	117
Hormone Response	1.5	3.3E-02	16	13	29	7.0	149	236	385	93.0	414
Steroid Receptor Signaling	1.8	3.2E-03	14	13	27	8.4	146	148	294	91.6	321
ALL	1.0	na	269	518	787	4.6	7,581	8,63	16,21	95.4	17,004

553 **Table 2. GSEA Functional Categories Enriched in Differentially Expressed Genes with**
554 **Enrichment Scores and Numbers of Up- or Down-Regulated Genes.** Enrichment scores were
555 calculated for each merged functional category using the ratio of the percent of differential genes in
556 the category compared to the percent of differential genes overall. (Overall 4% of 17,004 genes were
557 identified as differentially expressed using the filtering queries.)

558

559

560 **References**

561

- 562 1. Bull JH, Ellison G, Patel A, et al. Identification of potential diagnostic markers of prostate
563 cancer and prostatic intraepithelial neoplasia using cDNA microarray. *Br J Cancer*. Jun
564 2001;84(11):1512-9. doi:10.1054/bjoc.2001.1816
- 565 2. Welsh JB, Sapinoso LM, Su AI, et al. Analysis of gene expression identifies candidate markers
566 and pharmacological targets in prostate cancer. *Cancer Res*. Aug 2001;61(16):5974-8.
- 567 3. Peehl DM. Primary cell cultures as models of prostate cancer development. *Endocr Relat*
568 *Cancer*. Mar 2005;12(1):19-47. doi:10.1677/erc.1.00795
- 569 4. Sobel RE, Sadar MD. Cell lines used in prostate cancer research: a compendium of old and new
570 lines--part 1. *J Urol*. Feb 2005;173(2):342-59. doi:10.1097/01.ju.0000141580.30910.57
- 571 5. Goodspeed A, Heiser LM, Gray JW, Costello JC. Tumor-Derived Cell Lines as Molecular
572 Models of Cancer Pharmacogenomics. *Mol Cancer Res*. Jan 2016;14(1):3-13. doi:10.1158/1541-
573 7786.MCR-15-0189
- 574 6. Ellis WJ, Vessella RL, Buhler KR, et al. Characterization of a novel androgen-sensitive,
575 prostate-specific antigen-producing prostatic carcinoma xenograft: LuCaP 23. *Clin Cancer Res*. Jun
576 1996;2(6):1039-48.
- 577 7. van Weerden WM, de Ridder CM, Verdaasdonk CL, et al. Development of seven new human
578 prostate tumor xenograft models and their histopathological characterization. *Am J Pathol*. Sep
579 1996;149(3):1055-62.
- 580 8. Pretlow TG, Schwartz S, Giaconia JM, et al. Prostate cancer and other xenografts from cells in
581 peripheral blood of patients. *Cancer Res*. Aug 2000;60(15):4033-6.
- 582 9. Corey E, Quinn JE, Buhler KR, et al. LuCaP 35: a new model of prostate cancer progression to
583 androgen independence. *Prostate*. Jun 2003;55(4):239-46. doi:10.1002/pros.10198
- 584 10. Priolo C, Agostini M, Vena N, et al. Establishment and genomic characterization of mouse
585 xenografts of human primary prostate tumors. *Am J Pathol*. Apr 2010;176(4):1901-13.
586 doi:10.2353/ajpath.2010.090873
- 587 11. Raheem O, Kulidjian AA, Wu C, et al. A novel patient-derived intra-femoral xenograft model
588 of bone metastatic prostate cancer that recapitulates mixed osteolytic and osteoblastic lesions. *J Transl*
589 *Med*. Oct 28 2011;9:185. doi:10.1186/1479-5876-9-185
- 590 12. Godebu E, Muldong M, Strasner A, et al. PCSD1, a new patient-derived model of bone
591 metastatic prostate cancer, is castrate-resistant in the bone-niche. *J Transl Med*. Oct 3 2014;12:275.
592 doi:10.1186/s12967-014-0275-1
- 593 13. Nguyen HM, Vessella RL, Morrissey C, et al. LuCaP Prostate Cancer Patient-Derived
594 Xenografts Reflect the Molecular Heterogeneity of Advanced Disease and Serve as Models for
595 Evaluating Cancer Therapeutics. *Prostate*. May 2017;77(6):654-671. doi:10.1002/pros.23313
- 596 14. Navone NM, van Weerden WM, Vessella RL, et al. Movember GAP1 PDX project: An
597 international collection of serially transplantable prostate cancer patient-derived xenograft (PDX)
598 models. *Prostate*. 12 2018;78(16):1262-1282. doi:10.1002/pros.23701
- 599 15. Iype PT, Iype LE, Verma M, Kaighn ME. Establishment and characterization of immortalized
600 human cell lines from prostatic carcinoma and benign prostatic hyperplasia. *Int J Oncol*. Feb
601 1998;12(2):257-63. doi:10.3892/ijo.12.2.257
- 602 16. Karthaus WR, Iaquina PJ, Drost J, et al. Identification of multipotent luminal progenitor cells
603 in human prostate organoid cultures. *Cell*. Sep 2014;159(1):163-175. doi:10.1016/j.cell.2014.08.017

- 604 17. Drost J, Karthaus WR, Gao D, et al. Organoid culture systems for prostate epithelial and cancer
605 tissue. *Nat Protoc.* Feb 2016;11(2):347-58. doi:10.1038/nprot.2016.006
- 606 18. van de Wetering M, Francies HE, Francis JM, et al. Prospective derivation of a living organoid
607 biobank of colorectal cancer patients. *Cell.* May 2015;161(4):933-45. doi:10.1016/j.cell.2015.03.053
- 608 19. Sato T, Stange DE, Ferrante M, et al. Long-term expansion of epithelial organoids from human
609 colon, adenoma, adenocarcinoma, and Barrett's epithelium. *Gastroenterology.* Nov 2011;141(5):1762-
610 72. doi:10.1053/j.gastro.2011.07.050
- 611 20. Chua CW, Shibata M, Lei M, et al. Single luminal epithelial progenitors can generate prostate
612 organoids in culture. *Nat Cell Biol.* Oct 2014;16(10):951-61, 1-4. doi:10.1038/ncb3047
- 613 21. Agarwal S, Hynes PG, Tillman HS, et al. Identification of Different Classes of Luminal
614 Progenitor Cells within Prostate Tumors. *Cell Rep.* Dec 2015;13(10):2147-58.
615 doi:10.1016/j.celrep.2015.10.077
- 616 22. Gao D, Vela I, Sboner A, et al. Organoid cultures derived from patients with advanced prostate
617 cancer. *Cell.* Sep 2014;159(1):176-187. doi:10.1016/j.cell.2014.08.016
- 618 23. Puca L, Bareja R, Prandi D, et al. Patient derived organoids to model rare prostate cancer
619 phenotypes. *Nat Commun.* 06 2018;9(1):2404. doi:10.1038/s41467-018-04495-z
- 620 24. Beshiri ML, Tice CM, Tran C, et al. A PDX/Organoid Biobank of Advanced Prostate Cancers
621 Captures Genomic and Phenotypic Heterogeneity for Disease Modeling and Therapeutic Screening.
622 *Clin Cancer Res.* Sep 2018;24(17):4332-4345. doi:10.1158/1078-0432.CCR-18-0409
- 623 25. Richards Z, McCray T, Marsili J, et al. Prostate Stroma Increases the Viability and Maintains
624 the Branching Phenotype of Human Prostate Organoids. *iScience.* Feb 2019;12:304-317.
625 doi:10.1016/j.isci.2019.01.028
- 626 26. Tomlins SA, Rhodes DR, Perner S, et al. Recurrent fusion of TMPRSS2 and ETS transcription
627 factor genes in prostate cancer. *Science.* Oct 2005;310(5748):644-8. doi:10.1126/science.1117679
- 628 27. Hoffmann M, Kleine-Weber H, Schroeder S, et al. SARS-CoV-2 Cell Entry Depends on ACE2
629 and TMPRSS2 and Is Blocked by a Clinically Proven Protease Inhibitor. *Cell.* 04 2020;181(2):271-
630 280.e8. doi:10.1016/j.cell.2020.02.052
- 631 28. Hirata T, Park SC, Muldong MT, et al. Specific bone region localization of osteolytic versus
632 osteoblastic lesions in a patient-derived xenograft model of bone metastatic prostate cancer. *Asian J*
633 *Urol.* Oct 2016;3(4):229-239. doi:10.1016/j.ajur.2016.09.001
- 634 29. Lee S, Burner DN, Mendoza TR, et al. Establishment and Analysis of Three-Dimensional (3D)
635 Organoids Derived from Patient Prostate Cancer Bone Metastasis Specimens and their Xenografts. *J*
636 *Vis Exp.* Feb 3 2020;(156)doi:10.3791/60367
- 637 30. Pineda G, Lennon KM, Delos Santos NP, et al. Tracking of Normal and Malignant Progenitor
638 Cell Cycle Transit in a Defined Niche. *Sci Rep.* Apr 2016;6:23885. doi:10.1038/srep23885
- 639 31. Pappas KJ, Choi D, Sawyers CL, Karthaus WR. Prostate Organoid Cultures as Tools to
640 Translate Genotypes and Mutational Profiles to Pharmacological Responses. *J Vis Exp.* 10
641 2019;(152)doi:10.3791/60346
- 642 32. Crowell PD, Giafiglione JM, Hashimoto T, Diaz JA, Goldstein AS. Evaluating the
643 Differentiation Capacity of Mouse Prostate Epithelial Cells Using Organoid Culture. *J Vis Exp.* 11
644 2019;(153)doi:10.3791/60223
- 645 33. Hu WY, Hu DP, Xie L, Birch LA, Prins GS. Isolation of Stem-like Cells from 3-Dimensional
646 Spheroid Cultures. *J Vis Exp.* 12 2019;(154)doi:10.3791/60357
- 647 34. Tiriac H, French R, Lowy AM. Isolation and Characterization of Patient-derived Pancreatic
648 Ductal Adenocarcinoma Organoid Models. *J Vis Exp.* 01 2020;(155)doi:10.3791/60364

- 649 35. Fatehullah A, Tan SH, Barker N. Organoids as an in vitro model of human development and
650 disease. *Nat Cell Biol.* Mar 2016;18(3):246-54. doi:10.1038/ncb3312
- 651 36. Debnath J, Brugge JS. Modelling glandular epithelial cancers in three-dimensional cultures.
652 *Nat Rev Cancer.* Sep 2005;5(9):675-88. doi:10.1038/nrc1695
- 653 37. Lang SH, Stark M, Collins A, Paul AB, Stower MJ, Maitland NJ. Experimental prostate
654 epithelial morphogenesis in response to stroma and three-dimensional matrigel culture. *Cell Growth*
655 *Differ.* Dec 2001;12(12):631-40.
- 656 38. Vummidi Giridhar P, Williams K, VonHandorf AP, Deford PL, Kasper S. Constant
657 Degradation of the Androgen Receptor by MDM2 Conserves Prostate Cancer Stem Cell Integrity.
658 *Cancer Res.* 03 2019;79(6):1124-1137. doi:10.1158/0008-5472.CAN-18-1753
- 659 39. van Leenders GJ, Gage WR, Hicks JL, et al. Intermediate cells in human prostate epithelium
660 are enriched in proliferative inflammatory atrophy. *Am J Pathol.* May 2003;162(5):1529-37.
661 doi:10.1016/S0002-9440(10)64286-1
- 662 40. Liu X, Grogan TR, Hieronymus H, et al. Low CD38 Identifies Progenitor-like Inflammation-
663 Associated Luminal Cells that Can Initiate Human Prostate Cancer and Predict Poor Outcome. *Cell*
664 *Rep.* 12 2016;17(10):2596-2606. doi:10.1016/j.celrep.2016.11.010
- 665 41. Kröger C, Afeyan A, Mraz J, et al. Acquisition of a hybrid E/M state is essential for
666 tumorigenicity of basal breast cancer cells. *Proc Natl Acad Sci U S A.* 04 2019;116(15):7353-7362.
667 doi:10.1073/pnas.1812876116
- 668 42. Karthaus WR, Hofree M, Choi D, et al. Regenerative potential of prostate luminal cells revealed
669 by single-cell analysis. *Science.* 05 2020;368(6490):497-505. doi:10.1126/science.aay0267
- 670 43. Moradi F, Enjezab B, Ghadiri-Anari A. The role of androgens in COVID-19. *Diabetes Metab*
671 *Syndr.* Oct 2020;14(6):2003-2006. doi:10.1016/j.dsx.2020.10.014
- 672 44. Kyrou I, Karteris E, Robbins T, Chatha K, Drenos F, Randeve HS. Polycystic ovary syndrome
673 (PCOS) and COVID-19: an overlooked female patient population at potentially higher risk during the
674 COVID-19 pandemic. *BMC Med.* 07 2020;18(1):220. doi:10.1186/s12916-020-01697-5
- 675 45. McCoy J, Wambier CG, Vano-Galvan S, et al. Racial variations in COVID-19 deaths may be
676 due to androgen receptor genetic variants associated with prostate cancer and androgenetic alopecia.
677 Are anti-androgens a potential treatment for COVID-19? *J Cosmet Dermatol.* Jul 2020;19(7):1542-
678 1543. doi:10.1111/jocd.13455
- 679 46. Baratchian M, McManus JM, Berk M, et al. Sex, androgens and regulation of pulmonary AR,
680 TMPRSS2 and ACE2. *bioRxiv.* Oct 2020;doi:10.1101/2020.04.21.051201
- 681 47. Cadegiani FA, Goren A, Wambier CG. Spironolactone may provide protection from SARS-
682 CoV-2: Targeting androgens, angiotensin converting enzyme 2 (ACE2), and renin-angiotensin-
683 aldosterone system (RAAS). *Med Hypotheses.* Oct 2020;143:110112.
684 doi:10.1016/j.mehy.2020.110112
- 685 48. Mjaess G, Karam A, Aoun F, Albisinni S, Roumequère T. COVID-19 and the male
686 susceptibility: the role of ACE2, TMPRSS2 and the androgen receptor. *Prog Urol.* Sep
687 2020;30(10):484-487. doi:10.1016/j.purol.2020.05.007
- 688 49. Moutal A, Martin LF, Boinon L, et al. SARS-CoV-2 Spike protein co-opts VEGF-
689 A/Neuropilin-1 receptor signaling to induce analgesia. *Pain.* Oct
690 2020;doi:10.1097/j.pain.0000000000002097
- 691 50. Avanzato VA, Matson MJ, Seifert SN, et al. Case Study: Prolonged infectious SARS-CoV-2
692 shedding from an asymptomatic immunocompromised cancer patient. *Cell.* 2020;

693 51. Montopoli M, Zumerle S, Vettor R, et al. Androgen-deprivation therapies for prostate cancer
694 and risk of infection by SARS-CoV-2: a population-based study (N = 4532). *Ann Oncol.* 08
695 2020;31(8):1040-1045. doi:10.1016/j.annonc.2020.04.479
696